AD_____

Award Number: DAMD17-00-1-0646

TITLE: Gap Junctional Intercellular Communication and Breast Cancer Meatastasis to Bone

PRINCIPAL INVESTIGATOR: Henry J. Donahue, Ph.D.

CONTRACTING ORGANIZATION: The Pennsylvania State University
Hershey, Pennsylvania 17033-0850

REPORT DATE: October 2001

TYPE OF REPORT: Final

PREPARED FOR: U.S. Army Medical Research and Materiel Command
Fort Detrick, Maryland 21702-5012

DISTRIBUTION STATEMENT: Approved for Public Release;
Distribution Unlimited

The views, opinions and/or findings contained in this report are those of the author(s) and should not be construed as an official Department of the Army position, policy or decision unless so designated by other documentation.

20020909 039

REPORT DOCUMENTATION PAGE

Form Approved
OMB No. 074-0188

Public reporting burden for this collection of information is estimated to average 1 hour per response, including the time for reviewing instructions, searching existing data sources, gathering and maintaining the data needed, and completing and reviewing this collection of information. Send comments regarding this burden estimate or any other aspect of this collection of information, including suggestions for reducing this burden to Washington Headquarters Services, Directorate for Information Operations and Reports, 1215 Jefferson Davis Highway, Suite 1204, Arlington, VA 22202-4302, and to the Office of Management and Budget, Paperwork Reduction Project (0704-0188), Washington, DC 20503

1. AGENCY USE ONLY (Leave blank)	2. REPORT DATE	3. REPORT TYPE AND DATES COVERED
	October 2001	Final (1 Oct 00 - 30 Sep 01)

4. TITLE AND SUBTITLE
Gap Junctional Intercellular Communication and Breast Cancer Meatastasis to Bone

5. FUNDING NUMBERS
DAMD17-00-1-0646

6. AUTHOR(S)
Henry J. Donahue, Ph.D.

7. PERFORMING ORGANIZATION NAME(S) AND ADDRESS(ES)
The Pennsylvania State University
Hershey, Pennsylvania 17033-0850

E-Mail: hdonahue@psu.edu

8. PERFORMING ORGANIZATION REPORT NUMBER

9. SPONSORING / MONITORING AGENCY NAME(S) AND ADDRESS(ES)
U.S. Army Medical Research and Materiel Command
Fort Detrick, Maryland 21702-5012

10. SPONSORING / MONITORING AGENCY REPORT NUMBER

11. SUPPLEMENTARY NOTES
Report contains color

12a. DISTRIBUTION / AVAILABILITY STATEMENT
Approved for Public Release; Distribution Unlimited

12b. DISTRIBUTION CODE

13. ABSTRACT ***(Maximum 200 Words)***

This is the final report of a one year Concept Award. All three specific aims of the original proposal were successfully completed. We were also able to begin several additional experiments not proposed in the original application. We found that **1)** expressing the metastasis suppressing gene BRMS1 in diverse cancer cell lines, including breast and melanoma, restores homotypic gap junctional intercellular communication (GJIC); **2)** that metastatic breast cancer cells express a different connexin profile ($Cx43^-/Cx32^+$) than normal breast epithelial cells or metastases suppressed breast cancer cell lines ($Cx43^+/Cx32^-$); **3)** that metastatic breast cancer cells do not establish significant GJIC with normal breast epithelial cells but those expressing the metastasis suppressing gene BRMS1 do; **4)** that while metastatic breast cancer cells do not establish GJIC with themselves they do establish heterotypic GJIC with bone cells; **5)** that metastatic breast cancer cells express abundant OPN while those expressing the metastasis suppressing gene BRMS1 do not; and **6)** expressing Cx43 in metastatic breast cancer cells dramatically reduces OPN expression and reestablishes homotypic GJIC. These results suggest that connexin expression and GJIC contribute to breast cancer metastasis to bone.

14. SUBJECT TERMS	15. NUMBER OF PAGES
breast cancer, metastasis, gap junctions	35
	16. PRICE CODE

17. SECURITY CLASSIFICATION OF REPORT	18. SECURITY CLASSIFICATION OF THIS PAGE	19. SECURITY CLASSIFICATION OF ABSTRACT	20. LIMITATION OF ABSTRACT
Unclassified	Unclassified	Unclassified	Unlimited

Table of Contents

Introduction

Metastasis is a complex process by which tumor cells from one part of the body are able to leave their site of origin and move through the body to establish a new tumor at a distant site. In breast carcinomas, the distant tumors, known as metastases, are most commonly found in bone and lung. Although the cascade of events allowing the progression to occur remains unclear, several factors ranging from blood flow to cellular communication have been implicated.

This application proposes to examine the role of gap junctional intercellular communication (GJIC) in the metastatic process. Gap junctions are protein channels that allow adjacent cells to communicate with each other. GJIC may be homotypic, between cells of the same type, for instance tumor cell to tumor cell, or it may be heterotypic, between different cell types, for instance tumor cell and bone cell. In cancer progression, gap junctions are believed to play a significant role in both the initial formation of the primary tumor (tumorigenesis) as well as the formation of secondary, distant tumors (metastasis).

In breast cancer metastasis to bone, cancer cells must migrate through an osteoblastic bone lining cell layer prior to interacting with the bone extracellular matrix. This transosteoblastic migration requires cell-cell interactions that are poorly understood. Indeed, we are unaware of any studies examining the role of GJIC in this process.

We propose that because of the complex cascade of events occurring throughout cancer progression, GJIC changes. Our central hypothesis is that highly metastatic cells display decreased homotypic and heterotypic GJIC during tumorigenesis when compared to their less metastatic counterparts. Furthermore, highly metastatic cells display an increase in heterotypic GJIC during metastatic progression when compared to their metastatic counterparts.

Body

Specific Aim 1. Examine homotypic GJIC between metastatic 435 cells and themselves as well as metastasis suppressed 435/BrMS1 (435 cells transfected with the metastasis suppressing gene BrMS1) and themselves. Our hypothesis predicts that homotypic GJIC between 435 cells will be less than between 435/BrMS1 cells. We completed this specific aim and the results have been published in Saunders et al (appendix 1). Briefly, to examine homospecific GJIC, more than 450 individual 435 and 435pVC (vector controls for BrMS1 transfection) cells were analyzed by dual label fluorescent dye transfer in addition to 15 cells by direct injection of fluorescent dye. No evidence of homospecific GJIC between 435 and themselves or 435pVC and themselves was observed using either technique. More than 300 individual 435-BrMS1 cells were analyzed by double labeling and 8 cells by direct injection. Coupling was observed using double labeling and in 7 of 8 injected cells. From cell counting, it was estimated that a single injected cell transferred dye to more than 500 neighboring cells indicating coupling

was extensive. Thus, expressing the metastasis suppressing gene, BrMS1 in 435 cells restores GJIC as our hypothesis predicted.

In completing this specific aim we also examined expression of gap junction proteins (connexins) in breast cancer cells. We found that normal breast epithelial cells express the gap junction protein connexin (Cx) 43, but Cx32, was not detected. On the other hand, metsatic 435 cells expressed Cx32, but not Cx43 but metastasis suppressed 435/BrMS1 cells expressed Cx43 but Cx32. None of the breast cells examined expressed Cx26, Cx45 or Cx46. Thus expressing the metastasis suppressing gene BrMSD1 results in expression of a connexin profile more similar to normal breast epithelial cells than to metastatic cells suggesting that connexin expression is related to metastatic potential.

Specific Aim 2. Examine heterotypic GJIC between normal breast tissue cells and 435 or 435/BrMS1 to quantify the extent to which cells of varying metastatic potential are capable of communicating with healthy breast cells of the primary environment. Our hypothesis predicts that 435 cells will communicate less well with normal breast tissue cells than will 435/BrMS1. The absence of heterotypic GJIC may contribute to the ability of the metastatic 435 cells to maintain their transformed phenotype and is important in understanding the mechanisms that enable the primary tumor to grow and the cells to intially detach and metastasize. As a corollary, we will examine heterotypic GJIC between 435 and 435/BrMS1 to quantify the extent to which cells of a nonhomogenous tumor population are capable of communicating with each other. This is important in addressing the complexity of the tumor cell population in the *in vivo* environment. This aim has been completed and the results are detailed in Saunders et al (appendix 1). Briefly, metastasis-suppressed 435-BrMS1 cells coupled to non-tumorigenic, nonmetastatic HS578Bst breast epithelial cells. However, neither MDA 435 nor 435pVC cells formed functional gap junctions with HS578Bst cells. Likewise, MDA 435 and 435-BrMS1 cells were not capable of communicating with each other in any combination.

Specific Aim 3. Examine heterotypic GJIC between tumor cells (435 and 435/BrMS1) and a human osteoblastic cell line (hFOB) to quantify the extent to which cells of varying metastatic potential are capable of communicating with cells found in the secondary bone environment. The presence of heterotypic GJIC between the metastatic cells and osteoblastic cells may contribute to the specificity of tumor cells to localize to bone. As a control we will examine heterotypic GJIC between tumor cells and fibroblastic NIH 3T3 cells. Our hypothesis predicts that 435 cells will display greater GJIC with hFOB cells than will 435/BrMS1. We found that whereas 435 were not well coupled with themselves they displayed abundant heterotypic GJIC with osteoblastic hFOB cells. Indeed, 435 cells were approximately twice as well coupled to hFOB cells as were metastasis suppressed 435/BrMS1 cells. Thus, heterotypic GJIC between breast cancer cells and bone cells seems to be correlated to metastatic potential as our hypothesis predicted.

Timely completion of our initial specific aims has allowed us to examine other important issues regarding the role of gap junctions in breast cancer metastasis. We have examined

GJIC in another metastatic breast cancer cell line, MDA-MB-231 cells (231), as well as , the human melanoma cell lines MelJuSo and C8161.9, and these cells expressing BrMS1. We found that BrMS1 restored homotypic GJIC in 231, MelJuSo, and C8161.9 cells just as it did in 435 cells. This suggest that the effect of BrMS1 on GJIC is a generalized phenomena not restricted to a particular cancer cell type. These data have been published in Samant et al (appendix 2) and Shevede et al (appendix 3).

We have also had the opportunity to examine expression of genes associated with breast cancer metastasis in our cell lines. We first chose to examine osteopontin (OPN) expression. OPN is synthesized and secreted into the extracellular matrix by osteoblasts and has been implicated in cancer migration possibly by serving as a cancer cell chemoattractant. Our previous data suggested an inverse relationship between Cx43 and OPN expression in rat osteosarcoma (ROS) and human fetal osteoblastic (hFOB) cells. We found that OPN was undetectable in 435/BrMS1 cells but abundantly expressed in 435 and vector controls. Because of the inverse relationship between Cx43 OPN we and others have reported we next expressed Cx43 in 435 cells, which recall do not normally express Cx43, and examined OPN in these cells. We isolated 15 clones of 435 cells expressing Cx43 (435/Cx43$^+$). Real time RT-PCR revealed that Cx43 was detected in all 15 clones of 435/Cx43$^+$. Cx43 mRNA levels similar to 435/Cx43$^+$ were detected in hFOB cells and non-metastatic breast epithelial cells (Hs578). Liver tissue was used as positive control for Cx32 and negative control for OPN. OPN and Cx32 mRNA levels were decreased in 435/Cx43$^+$ cells relative to 435 or vector controls but were still greater than in hFOB cells and Hs578. Homotypic GJIC between 435/Cx43$^+$ cells was increased 5 to 8.5 fold relative to GJIC between vector controls or wild type 435 cells. Heterotypic coupling between 435/Cx43$^+$ and hFOB cells increased 1.5 to 3 fold relative to that between vector controls or wild type 435 cells and hFOB cells. Taken together these results suggest an inverse relationship between Cx43 expression and metastatic potential of breast cancer cells. Furthermore, since breast cancer cells which do and do not express Cx43 appear to express different metastatic potentials and since heterotypic GJIC between these cells and osteoblastic cells differ, we suggest that alteration in GJIC may be related to breast cancer cell metastasis to bone. These data will be presented at the 2002 meetings of the Orthopaedic Research Society and the American Association of Cancer Research (appendices 4 and 5, respectively).

Key Research Accomplishments

- Discovered that expressing the metastasis suppressing gene in diverse cancer cell lines, including breast and melanoma, restores homotypic GJIC.
- Discovered that metastatic breast cancer cells express a different connexin profile (Cx43$^-$/Cx32$^+$) than normal breast epithelial cells or metastases suppressed breast cancer cell lines (Cx43$^+$/Cx32$^-$).
- Discovered that metastatic breast cancer cells do not establish significant GJIC with normal breast epithelial cells but those expressing the metastasis suppressing gene BrMS1 do.
- Discovered that while metastatic breast cancer cells do not establish GJIC with themselves they do establish heterotypic GJIC with bone cells.

- Discovered that metastatic breast cancer cells express abundant OPN while those expressing the metastasis suppressing gene BrMS1 do not.
- Expressing Cx43 in metastatic breast cancer cells dramatically reduces OPN expression and reestablishes homotypic GJIC.

Reportable outcomes

Manuscripts

1. Saunders, M.M., Li, Z., Winter, C.R., Seraj, M.J., Welch, D.R., Donahue, H.J. (2001) Breast cancer metastatic potential correlates with a break down in homospecific and heterospecific gap junctional intercellular communication. Cancer Research 61(5)1765-1767.

2. Samant, R.S., Seraj, M. J., Saunders, M. M , Sakamaki, T. S., Shevde, L. A, Harms, J. F., Leonard, T. O., Goldberg, S. F., Budgeon, L., Meehan, W. J., Winter, C. R., Christensen, N. D., Verderame, M. F., Donahue, H. J., Welch, D. R (2001) *BRMS1* suppresses human breast carcinoma metastasis by inhibiting motility and restoring gap junctional intercellular communication. Clinical and Experimental Metastasis 18(8):683-693.

3. Shevde, L.A., Samant, R.S., Goldberg, S.F., Sikaneta, T., Alessandrini, A., Donahue, H.J., Mauger, D.T., Welch, D.R. (2002) Suppression of human melanoma metastasis by the metastasis suppressor gene, BRSM1. Experimental Cell Research (in press).

Abstracts

1. Saunders, M.M., Seraj, M.J.,Yellowley, C.E., Hoke, A., Welch, D.R., and Donahue, H.J. (2000) Gap junctional intercellular communication is restored in metastasis suppressed breast carcinoma cells. Experimental Biology 2000.

2. Seraj, M.J., Samant, R.S., Shevde, L.A., Saunders, M.M., Sakamaki, T., Meehan, W.J., Donahue, H.J., Debies, M.T., Budgeon, L., Leonard, T.O., Harms, J.F., Christensen, N.D., Winter, C.R., Verderame, M.F., and Welch, D.R. (2000) BRMS1- a human breast cancer metastasis suppressor gene encoded on chromosome 11q13.1-q13.2. Era of Hope- Department of Defense Breast Cancer Research Program Meeting 1: 111-112.

3. Saunders, M.M., Li, Z., Winter, C.R., Welch, D.R. and Donahue, H.J. (2000) Metastatic breast carcinoma correlates with a breakdown in gap junction function and expression. Clinical and Experimental Metastasis 17: P50.

4. Saunders, M.M., Kunze, E., Li, Z., Mastro, A., and Donahue H.J. (2001) Quantification and characterization of gap junctions and gap junctional

intercellular communication in an in vitro breast carcinoma model metastatic to bone. 47th Annual Meeting, Transaction of the Orthopaedic Research Society, Vol.26.

5. Li, Z., Zhou, Z., Saunders, M.M., Casey, G., Welch, D.R., Donahue, H.J. (2001) Connexin and osteopontin expression correlate with breast cancer metastatic potential. Proceedings of the American Association for Cancer Research 42: 4244.

Funding

Successful completion of this project has enabled us to obtain funding from the National Institutes of Health to continue this work:

Intercellular communication in breast cancer metastasis to bone, NIH, R01CA90991-01, $1,277,370 for five years, 4/01/01-3/31/06, 20% effort.

Conclusions

Our results suggest that connexin expression and GJIC contribute to breast cancer metastasis to bone. Successful completion of the project has allowed us to obtain funding to continue the project. We are currently examining the mechanisms by which connexin expression and GJIC contribute to breast cancer metastatic potential. We have recently injected Cx43 expressing breast cancer cell into athymic nude mice to assess metastasis in vivo. If we find that Cx43 expression does indeed reduce breast cancer metastasis it would suggest a novel and very exiting target for metastasis therapy.

[CANCER RESEARCH 61, 1765–1767, March 1, 2001]

Donahue
Appendix 1

Advances in Brief

Breast Cancer Metastatic Potential Correlates with a Breakdown in Homospecific and Heterospecific Gap Junctional Intercellular Communication[1]

Marnie M. Saunders,[2] M. Jabed Seraj, Zhongyong Li, Zhiyi Zhou, Cathy R. Winter, Danny R. Welch, and Henry J. Donahue

Departments of Orthopaedics and Rehabilitation [M. M. S., Z. L., Z. Z., H. J. D.] and Cellular and Molecular Physiology [H. J. D.] and Jake Gittlen Cancer Research Institute [C. R. W., D. R. W.], The Pennsylvania State University College of Medicine, The Milton S. Hershey Medical Center, Hershey, Pennsylvania 17033, and Department of Urology, University of Virginia, Charlottesville, Virginia 22908 [M. J. S.]

Abstract

Breast cancer progresses toward increasingly malignant behavior in tumorigenic and metastatic stages. In the series of events in the metastatic stage, tumor cells leave the primary tumor in breast and travel to distant sites where they establish secondary tumors, or metastases. In this report, we demonstrate that cell-cell communication via gap junctions is restored in the metastatic human breast carcinoma cell line MDA-MB-435 when it is transfected with breast metastasis suppressor 1 (BRMS1) cDNA. Furthermore, the expression profile of connexins (Cxs), the protein subunits of gap junctions, changes. Specifically, the expression of BRMS1 in MDA-MB-435 cells increases Cx43 expression and reduces Cx32 expression, resulting in a gap junction phenotype more similar to normal breast tissue. Taken together, these results suggest that gap junctional communication and the Cx expression profile may contribute to the metastatic potential of these breast cancer cells.

Introduction

GJIC[3] has been linked previously to tumorigenesis (1, 2) and progression toward metastasis (3–5). Gap junctions are membrane-spanning channels composed of protein subunits called Cxs that facilitate GJIC by allowing small (M_r <1000) signaling molecules to pass from cell to cell. GJIC may be homospecific, coupling cells of the same type, or heterospecific, coupling cells of unlike type (6). In tumorigenesis, a breakdown in homospecific and heterospecific coupling has been demonstrated to precede neoplasia and has been hypothesized as necessary to maintain malignant phenotype transformation (2). We propose that this breakdown in communication also contributes to metastatic potential in human breast carcinoma cells. To explore this possibility, we examined the hypothesis that metastatic potential correlates with gap junction expression and function quantified *in vitro*. The breast cancer model we used compared MDA-MB-435 cells (MDA 435) and these cells expressing the recently described metastasis suppressor gene, *BRMS1* (435-BRMS1; Ref. 7). MDA 435 and 435-BRMS1 cells provide a powerful model to study metastasis because they have genetically identical backgrounds, thus reducing biological noise otherwise present when comparing genetically unrelated heterologous tumor cell lines. In this study, we demonstrate that introduction of BRMS1 cDNA reestablishes both homospecific and heterospecific GJIC function and alters the pattern of gap junction protein (Cx) expression.

Received 11/2/00; accepted 1/11/01.

The costs of publication of this article were defrayed in part by the payment of page charges. This article must therefore be hereby marked *advertisement* in accordance with 18 U.S.C. Section 1734 solely to indicate this fact.

[1] This work was supported by Grants AG13087 and CA87728 from the NIH, Grant BC995879 from the United States Army, and a grant from the National Foundation for Cancer Research.

[2] To whom requests for reprints should be addressed, at Musculoskeletal Research Laboratory, Department of Orthopaedics and Rehabilitation, The Pennsylvania State University College of Medicine, P. O. Box 850, 500 University Drive, Hershey, PA 17033. Phone: (717) 531-4818; Fax: (717) 531-7583.

[3] The abbreviations used are: GJIC, gap junctional intercellular communication; Cx, connexin; BRMS1, breast metastasis suppressor 1.

Materials and Methods

Cell Culture. Four cell lines were used in this study. The metastatic cell line MDA 435 was derived from pleural effusion from a female patient with an infiltrating ductal carcinoma (8). 435-BRMS1 are MDA 435 cells transfected with BRMS1 cDNA driven by the CMV promoter (7). 435pVC are MDA 435 cells expressing plasmid vector (pcDNA3; Invitrogen, Carlsbad, CA) only and served as a control for transfections (7). HS578Bst is an immortalized nontumorigenic, nonmetastatic breast epithelial cell line (9) purchased from American Type Culture Collection. They were used to represent normal breast epithelial cells. The MDA 435 cell line was maintained in DMEM/F12 cell culture medium (Life Technologies, Inc., Rockville, MD) containing 5% fetal bovine serum. 435pVC and 435-BRMS1 lines were maintained in this same medium supplemented with geneticin (500 μg/ml). HS578Bst cells were maintained in DMEM (Life Technologies) supplemented with 10% fetal bovine serum and epidermal growth factor (30 ng/ml). Cells were passaged using a 2 mM EDTA solution in calcium- and magnesium-free Dulbecco's PBS.

Assessment of GJIC. To corroborate GJIC assays, two complimentary techniques were used, as described previously (10). Homospecific and heterospecific GJIC were functionally assessed using double labeling fluorescent dye transfer assays (11) and direct cell injections (10). Homospecific coupling was assessed for the three tumorigenic cell lines: MDA 435, 435pVC, and 435-BRMS1. Heterospecific coupling was assessed among the three tumorigenic cell lines in all possible combinations, as well as with the nontumorigenic, nonmetastatic human breast line, HS578Bst.

For double labeling assays, "acceptor" cells were plated at a density of 4×10^4 cells/cm^2 to round (25-mm) glass coverslips placed previously in round (35-mm) polystyrene Petri dishes. Cells were allowed to reach 90% confluence at 37°C in a humidified CO_2 incubator over a period of 24–48 h. Simultaneously, "donor" cells were plated at a density of 4×10^4 cells/cm^2 in 35-mm tissue culture dishes and maintained at 37°C over the same time period. GJIC was quantified as described previously (12). Briefly, donor cells were labeled with a fluorescent dye mixture containing calcein AM (Molecular Probes, Eugene, Oregon) and 1,1′-dioctadecyl-3,3,3′,3′-tetramethylindocarbocyanine perchlorate (Molecular Probes), detached, centrifuged, resuspended in fresh growth medium, and counted using a hemacytometer. Double-labeled donor cells were then dropped onto confluent monolayers of unlabeled acceptor cells at a ratio of approximately 1:500 (labeled:unlabeled) cells and incubated for 90 min at 37°C. After incubation, the coverslips were removed from the dishes, washed twice with room temperature PBS, and inverted onto clean, glass microscope slides and evaluated using a Nikon epifluorescence microscope (Nikon EFD-3; Optical Apparatus Co., Ardmore, PA). Calcein, because of its small molecular size (M_r 994,870), diffuses to neighboring cells via GJIC. The fluorescent dye, 1,1′-dioctadecyl-3,3,3′,3′-tetramethylindocarbocyanine perchlorate, intercalates within cell membranes and does not transfer to neighboring cells via GJIC but is used to visualize the donor cell.

For direct cell injections, cells were plated at a density of 3.5×10^4 cells/cm^2 on round (25-mm) glass coverslips in tissue culture dishes and examined at 90% confluence. Cells were washed twice with room temperature PBS and sandwiched in a metal and nylon well affixed to the fluorescent microscope and submerged in room temperature PBS throughout the duration of the experiment. Individual cells were impaled with glass micropipettes that had been backfilled with a fluorescent dye mixture of Lucifer yellow (Molecular Probes) dissolved in lithium chloride. Cells were impaled 3 min, the

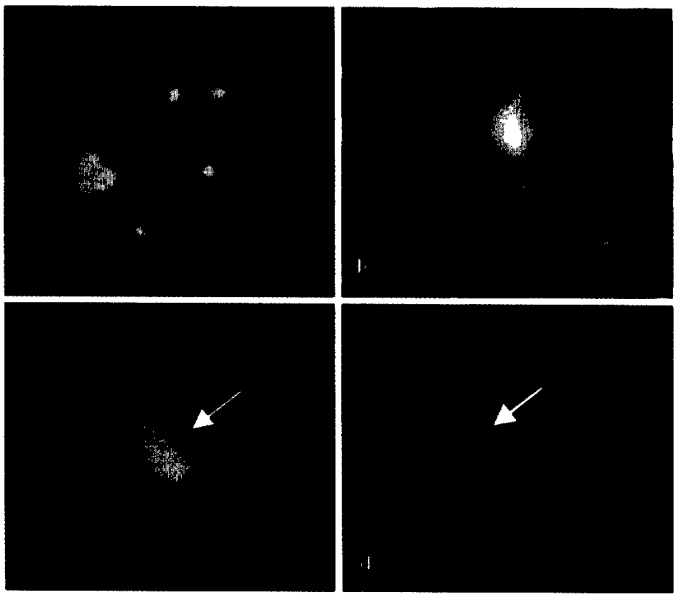

Fig. 1. Homospecific GJIC in breast cancer cell lines. Parent MDA 435 (*a*) or 435-BRMS1 (*b*) were grown in monolayer and subjected to double labeling assays. Calcein-loaded MDA 435 donor cells were placed in contact with monolayer MDA 435 acceptor cells (*a*), and calcein-loaded 435-BRMS1 donor cells were placed in contact with monolayer 435-BRMS1 acceptor cells (*b*). Neither MDA 435 nor 435pVC displayed homospecific GJIC, whereas 435-BRMS1 did. Individual MDA 435 (*c*) or 435-BRMS1 (*d*) cells were injected with Lucifer yellow. Dye remained within MDA 435 cells but transferred from the injected 435-BRMS1 to neighboring 435-BRMS1, indicating homospecific coupling within an elapsed time of 5 min. ×400. *Arrows*, injected cells.

pipette was removed, and dye transfer was monitored for an additional 2 min. In preliminary experiments, it was found that 435-BRMS1 cells did not adhere firmly to glass substrates. Therefore, in an attempt to optimize cell attachment, we plated 435-BRMS1 cells onto coverslips coated with collagen type I (10 $\mu g/cm^2$) and type II (.5 mg/ml), fibronectin (10 $\mu g/cm^2$), Matrigel (1 mg/ml), Cell-tak (1 mg/ml), poly-D-lysine (5 $\mu g/cm^2$), and poly-L-lysine (5 $\mu g/cm^2$) purchased from Becton Dickinson (Bedford, MA). We found that poly-D-lysine coating provided optimal conditions for our experiments; therefore, all experiments reported are from cells plated on poly-D-lysine.

Northern Blot Analysis of Cx mRNA Expression. Steady-state mRNA levels of the gap junction proteins Cx26, Cx32, Cx43, Cx45, and Cx46 were quantified by Northern blot analysis for all four cell lines examined. Cells were plated at a density of 2×10^4 cells/cm^2 in 100-mm tissue culture dishes and cultured to confluence, and total RNA was isolated as described (11). Briefly, total RNA (20 μg), as determined by absorption at 260 nm, was subjected to electrophoresis on a 1% agarose formaldehyde gel. The gels were then capillary blotted with 100 mM sodium phosphate onto membranes (Gene Screen Hybridization Transfer Membrane; DuPont NEN) and prehybridized for 15 min at 55°C in 1% BSA, 350 mM sodium phosphate, 7% SDS, and 30% (v/v) deionized formamide and followed by hybridization overnight in the same solution with [α-^{32}P]dCTP-labeled probes for the 1.3-kb coding region of Cx43 cDNA, the entire 1.2-kb coding region of Cx45 cDNA, an *Eco*RI fragment of rat Cx46 cDNA, a 1.1-kb *Hin*cII-*Bst* fragment of Cx26 cDNA, a full-length 1.5-kb cDNA for Cx32 cDNA, or a 1.4-kb *Pst*I fragment of rat glyceraldehyde 3-phosphate dehydrogenase cDNA. The blots were washed once in 150 mM sodium phosphate and 0.1% SDS at room temperature, followed by two washings at 55°C.

Results

Quantification of Dye Coupling. To examine homospecific GJIC, >450 individual 435 and 435pVC cells were analyzed by double labeling in addition to 15 cells by direct injection. No evidence of homospecific GJIC was observed using either technique. Fig. 1*a* shows a plate of 435 cells in monolayer (black) with the double-labeled cells shown in yellow in the dual exposure photograph (×400). As evidenced by the lack of dye transfer, MDA 435 cells were not functionally coupled and therefore not able to communicate with themselves via gap junctions. This was corroborated with the direct cell injection technique, in which Lucifer yellow remained in the injected cell and did not spread (Fig. 1*c*). More than 300 individual 435-BRMS1 cells were analyzed by double labeling, and 8 cells were analyzed by direct injection. Coupling was observed using double labeling (Fig. 1*b*, note donor cells appear yellow, whereas neighboring acceptor cells appear green) and in seven of eight injected cells (Fig. 1*d*, note that both the injected cell and neighboring cells appear yellow). From cell counting, it was estimated that a single injected cell transferred dye to >500 neighboring cells, indicating that coupling was extensive.

We next examined heterospecific GJIC. For each experimental condition, >90 cells were examined. Metastasis-suppressed 435-BRMS1 cells coupled to nontumorigenic, nonmetastatic breast HS578Bst cells. However, neither MDA 435 nor 435pVC cells formed functional gap junctions with HS578Bst cells. Likewise, MDA 435 and 435-BRMS1 cells were not capable of communicating with each other in any combination (data not shown).

Expression of Cx mRNA. We did not detect mRNA for Cx26, Cx45, or Cx46 (data not shown) in any of the cell lines examined. However, Cx43 mRNA was highly expressed in HS578Bst cells and 435-BRMS1 cells, albeit less abundantly in the latter. On the other hand, Cx43 mRNA was not detected in MDA 435 or 435pVC cells (Fig. 2). Interestingly, although Cx32 mRNA was highly expressed in 435 and 435pVC, it was not detected in HS578Bst and 435-BRMS1 cells (Fig. 3). These findings were consistent with three separate experiments.

Discussion

In this study, we examined gap junction function and expression in related breast carcinoma cell lines having varying metastatic potentials. Although metastatic MDA 435 cells did not form homospecific GJIC under the *in vitro* conditions described, metastasis-suppressed 435-BRMS1 cells displayed abundant homospecific GJIC with neighboring cells. Thus, re-expression of the metastasis-suppressor BRMS1 reestablishes GJIC in 435 cells. Likewise, MDA 435 cells did not

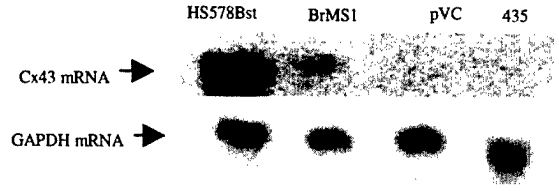

Fig. 2. Cx43 mRNA expression in human breast epithelial cells and breast cancer cell lines. Cells were cultured to confluence and steady-state Cx43 (*upper panel*) and GAPDH (*lower panel*) mRNA levels assessed by Northern blot analysis. Neither metastatic MDA 435 or 435pVC (pcDNA3-transfected) cells expressed Cx43. Human breast epithelial cells (HS578Bst) expressed Cx43, and Cx43 was moderately expressed in the metastasis-suppressed 435-BRMS1 cells. This result is typical of three similar experiments.

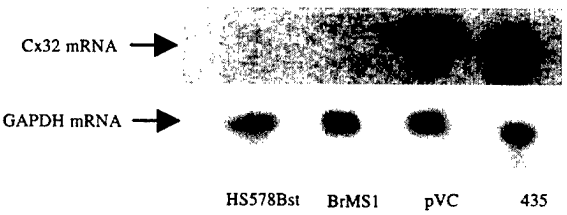

Fig. 3. Cx32 mRNA expression in human breast epithelial cells and breast cancer cell lines. Cells were cultured to confluence, and steady-state Cx32 (*upper panel*) and GAPDH (*lower panel*) mRNA levels were assessed by Northern blot analysis. Neither human breast epithelial cells (HS578Bst) nor metastasis-suppressed 435-BRMS1 cells expressed Cx32. Both MDA 435 and 435pVC expressed Cx32. This result is typical of three similar experiments.

form functional gap junctions with breast epithelial cells (HS578Bst). Yet, metastasis-suppressed 435-BRMS1 cells did. Taken together, these findings support the notion that disruption of breast carcinoma-breast carcinoma or breast carcinoma-breast epithelial cell GJIC contributes to metastatic potential. That 435-BRMS1 cells (tumorigenic, poorly metastatic) form gap junctions with HS578Bst cells suggests that alteration in gap junctions is a later event in tumor progression, at least in the MDA 435 model.

Cx43 is the predominant gap junction protein in normal breast epithelial tissue (13), but the expression of Cx26 in normal breast epithelial tissue is less clear. Some groups have failed to detect Cx26 in normal mammary tissue, whereas other groups have (14, 15). The expression of other Cxs, including Cx32, has not been reported in human breast tissue, but in mice Cx26 and Cx32 have been reported in breast tissue during pregnancy and lactation, respectively (16).

In the HS578Bst breast epithelium-derived cells, Cx43, but not Cx26 or Cx32, was expressed. On the other hand, metastatic MDA 435 cells expressed neither Cx26 nor Cx43, consistent with the loss of Cx43 expression reported in neoplastic breast tissue (15), but did express Cx32. Restoring BRMS1 expression results in reestablishment of GJIC but only partly restored Cx43 expression. This suggests the possibility of novel Cxs in 435-BRMS1 cells or, more likely, that a relatively low level of Cx43 expression is sufficient for establishing detectable GJIC. A more striking finding was that although metastatic MDA 435 cells expressed Cx32, metastasis-suppressed 435-BRMS1 cells did not. To our knowledge, Cx32 has not been thoroughly examined in tumorigenic and metastatic breast cancer cells. To date, the only study examining Cx32 in neoplastic tissue failed to detect it in breast carcinoma (15). Our data suggest that re-expression of the metastasis-suppressor gene *BRMS1* returns the Cx expression profile from that of a metastatic cell (Cx32 but not Cx43) to that more similar to a normal breast epithelial cell (Cx43 but not Cx32). Furthermore, although BRMS1 expression restores, at least in part, Cx43 mRNA expression, it may inhibit Cx32 mRNA expression. At minimum, these data imply that the composition of gap junctions contributes to metastatic propensity. It is also possible, although more extensive studies are required, that Cx32 expression contributes to breast cancer cell metastatic potential.

The mechanism by which altered Cx expression and GJIC might contribute to metastasis is unclear. One possibility is that deficient heterospecific GJIC between cancer cells and normal breast epithelial cells contributes to detachment of the malignant cells from the primary tumor. This concept is supported by studies showing a relationship between E-cadherin, a cell-cell adhesion molecule that is down-regulated in many tumors (17), and gap junction expression and function (18). However, none of the MDA 435 variants express E-cadherin (7), suggesting that E-cadherin may contribute to tumorigenesis but not metastatic potential. This does not preclude the possibility that altered Cx expression and GJIC may regulate other cell adhesion molecules that could contribute to the detachment of malignant cells from the primary tumor.

Another mechanism by which altered Cx expression and GJIC might contribute to metastatic potential is by facilitating arrest on, or colonization of, the secondary tumor environment. For instance, GJIC has been demonstrated between metastatic tumor cells and vascular endothelium (19) and is directly related to metastatic potential (20). Recently, Ito *et al.* (3) demonstrated that B16-BL6 melanoma cells, which are metastatic after s.c. injection, expressed Cx26 and displayed GJIC with endothelial cells. However, B16-F10 melanoma cells, which did not metastasize after s.c. injection in their hands, did not express Cx26, nor did they establish GJIC with endothelial cells. Transfection with wild-type Cx26 made F10 cells as competent to communicate with endothelial cells as B16-BL6 cells. Conversely, transfection with a dominant-negative form of Cx26 rendered B16-BL6 cells deficient in GJIC and less metastatic. Taken together, these results suggest that heterospecific GJIC between tumor cells and endothelial cells, or other cells in the secondary tumor environment, may contribute to the metastatic potential of malignant cells. Future studies will address these possibilities.

In summary, the experiments presented here demonstrate two things: (*a*) they show that restoration of BRMS1 expression in MDA 435 cells results in concomitant reduction in metastatic efficiency and restoration of GJIC; and (*b*) BRMS1 expression alters Cx expression in the tumor cells. Together these findings imply that BRMS1 is acting by a novel mechanism to inhibit metastasis, and that GJIC mediated by specific Cxs may be a major determinant of metastatic potential in human breast cancer.

Acknowledgments

We acknowledge Dr. Clare Yellowley for technical assistance with the direct cell injections.

References

1. Loewenstein, W. R., and Kanno, Y. Intercellular communication and the control of tissue growth: lack of communication between cancer cells. Nature (Lond.), *209:* 1248–1249, 1966.
2. Yamasaki, H., Mesnil, M., Omori, Y., Mironov, N., and Krutovskikh, V. Intercellular communication and carcinogenesis. Mutat. Res., *333:* 181–188, 1995.
3. Ito, A., Katoh, F., Kataoka, T. R., Okada, M., Tsubota, N., Asada, H., Yoshikawa, K., Maeda, S., Kitamura, Y., Yamasaki, H., and Nojima, H. A role for heterologous gap junctions between melanoma and endothelial cells in metastasis. J. Clin. Investig., *105:* 1189–1197, 2000.
4. El-Sabban, M. E., and Pauli, B. U. Cytoplasmic dye transfer between metastatic tumor cells and vascular endothelium. J. Cell Biol., *115:* 1375–1381, 1991.
5. Nicolson, G. L., Dulski, K. M., and Trosko, J. E. Loss of intercellular junctional communication correlates with metastatic potential in mammary adenocarcinoma cells. Proc. Natl. Acad. Sci. USA, *85:* 473–476, 1988.
6. Trosko, J., and Ruch, R. Cell-cell communication in carcinogenesis. Frontiers Biosci., *3:* d208–d236, 1998.
7. Seraj, M. J., Samant, R. S., Verderame, M. F., and Welch, D. R. Functional evidence for a novel human breast carcinoma metastasis suppressor, BRMS1, encoded at chromosome 11q13. Cancer Res., *60:* 2764–2769, 2000.
8. Price, J. E., Polyzos, A., Zhang, R. D., and Daniels, L. M. Tumorigenicity and metastasis of human breast carcinoma cell lines in nude mice. Cancer Res., *50:* 717–721, 1990.
9. Hackett, A. J., Smith, H. S., Springer, E. L., Owens, R. B., Nelson-Rees, W. A., Riggs, J. L., and Gardner, M. B. Two syngeneic cell lines from human breast tissue: the aneuploid mammary epithelial (Hs578T) and the diploid myoepithelial (Hs578Bst) cell lines. J. Natl. Cancer Inst., *58:* 1795–1806, 1977.
10. Vander Molen, M. A., Rubin, C. T., McLeod, K. J., McCauley, L. K., and Donahue, H. J. Gap junctional intercellular communication contributes to hormonal responsiveness in osteoblastic networks. J. Biol. Chem., *271:* 12165–12171, 1996.
11. Donahue, H. J., Li, Z., Zhou, Z., and Yellowley, C. E. Differentiation of human fetal osteoblastic cells is partially dependent on gap junctional intercellular communication. Am. J. Physiol. Cell Physiol. *278:* C315–C322, 2000.
12. Yellowley, C. E., Li, Z., Zhou, Z., Jacobs, C. R., and Donahue, H. J. Functional gap junctions between osteocytic and osteoblastic cells. J. Bone Miner. Res., *15:* 209–217, 2000.
13. Cai, J., Jiang, W. G., and Mansel, R. E. Gap junctional communication and the tyrosine phosphorylation of connexin 43 in interaction between breast cancer and endothelial cells. Int. J. Mol. Med., *1:* 273–278, 1998.
14. Hirschi, K. K., Xu, C. E., Tsukamoto, T., and Sager, R. Gap junction genes *Cx26* and *Cx43* individually suppress the cancer phenotype of human mammary carcinoma cells and restore differentiation potential. Cell Growth Differ., *7:* 861–870, 1996.
15. Wilgenbus, K. K., Kirkpatrick, C. J., Knuechel, R., Willecke, K., and Traub, O. Expression of Cx26, Cx32 and Cx43 gap junction proteins in normal and neoplastic human tissues. Int. J. Cancer, *51:* 522–529, 1992.
16. Locke, D., Perusinghe, N., Newman, T., Jayatilake, H., Evans, W. H., and Monaghan, P. Developmental expression and assembly of connexins into homomeric and heteromeric gap junction hemichannels in the mouse mammary gland. J. Cell Physiol., *183:* 228–237, 2000.
17. Berx, G., Becker, K. F., Hofler, H., and van Roy, F. Mutations of the human E-cadherin (*CDH1*) gene. Hum. Mutat., *12:* 226–237, 1998.
18. Jongen, W. M. F., Fitzgerald, D. J., Asamoto, M., Piccoli, C., Slaga, T. J., Gros, D., Takeichi, M., and Yamasaki, H. Regulation of connexin 43-mediated gap junctional intercellular communication by Ca^{2+} in mouse epidermal cells is controlled by E-cadherin. J. Cell Biol., *114:* 545–555, 1991.
19. El-Sabban, M. E., and Pauli, B. U. Adhesion-mediated gap junctional communication between lung-metastatic cancer cells and endothelium. Invasion Metastasis, *14:* 164–176, 1994.
20. Brauner, T., and Hulser, D. F. Tumor cell invasion and gap junctional communication. II. Normal and malignant cells confronted in multicell spheroids. Invasion Metastasis, *10:* 31–48, 1990.

Clinical & Experimental Metastasis **18:** 683–693, 2001.
© 2001 *Kluwer Academic Publishers. Printed in the Netherlands.*

Analysis of mechanisms underlying *BRMS1* suppression of metastasis

R.S. Samant[1], M.J. Seraj[1,4], M.M. Saunders[2], T.S. Sakamaki[1], L.A. Shevde[1], J.F. Harms[1], T.O. Leonard[1], S.F. Goldberg[1], L. Budgeon[1], W.J. Meehan[1], C.R. Winter[1], N.D. Christensen[1], M.F. Verderame[3], H.J. Donahue[2] & D.R. Welch[1]

[1]*Jake Gittlen Cancer Research Institute, Musculoskeletal Research Laboratory,* [2]*Department of Orthopaedics and Rehabilitation and* [3]*Department of Medicine, The Pennsylvania State University College of Medicine, Hershey, Pennsylvania, USA;* [4]*Present address: Department of Urology, University of Virginia, Charlottesville, Virginia, USA*

Received 8 May 2001; accepted in revised form 6 July 2001

Key words: breast cancer, chromosome 11q13, gap junctions, metastasis suppressor gene, motility

Abstract

Introduction of normal, neomycin-tagged human chromosome 11 (neo11) reduces the metastatic capacity of MDA-MB-435 human breast carcinoma cells by 70–90% without affecting tumorigenicity. Differential display comparing MDA-MB-435 and neo11/435 led to the discovery of a human breast carcinoma metastasis suppressor gene, *BRMS1*, which maps to chromosome 11q13.1–q13.2. Stable transfectants of MDA-MB-435 and MDA-MB-231 breast carcinoma cells with BRMS1 cDNA still form progressively growing, locally invasive tumors when injected in mammary fat pads of athymic mice but exhibit significantly lower metastatic potential (50–90% inhibition) to lungs and regional lymph nodes. To begin elucidating the mechanism(s) of action, we measured the ability of BRMS1 to perturb individual steps of the metastatic cascade modeled *in vitro*. Consistent differences were not observed for adhesion to extracellular matrix components (laminin, fibronectin, type IV collagen, type I collagen, Matrigel); growth rates *in vitro* or *in vivo*; expression of matrix metalloproteinases, heparanase, or invasion. Likewise, BRMS1 expression did not up regulate expression of other metastasis suppressors, such as NM23, Kai1, KiSS1 or E-cadherin. Motility of BRMS1 transfectants was modestly inhibited (30–60%) compared to parental and vector-only transfectants. Ability to grow in soft agar was also decreased in MDA-MB-435 cells by 80–89%, but the decrease for MDA-MB-231 was less (13–15% reduction). Also, transfection and re-expression of BRMS1 restored the ability of human breast carcinoma cells to form functional homotypic gap junctions. Collectively, these data suggest that BRMS1 suppresses metastasis of human breast carcinoma by complex, atypical mechanisms.

Abbreviations: BAC – bacterial artificial chromosome; BRMS1 – breast cancer metastasis suppressor 1; CMF-DPBS – calcium and magnesium free Dulbecco's phosphate buffered saline; DAPI – 4′,6-diamidino-2-phenylindole; DD-RT-PCR – differential display; DME-F12 – mixture (1:1) Dulbecco's -modified minimum essential medium and Ham's F-12 medium; FISH – fluorescence in situ hybridization; G-418 – Geneticin; GJIC – gap junctional intercellular communication; HBSS – Hank's balanced salt solution; SDS sodium dodecyl sulfate; PAGE – poly acrylamide gel electrophoresis, P_i – inorganic phosphate; TE – 0.125% trypsin – 2 mM EDTA solution in CMF-DPBS; TTBS – Tris-buffered saline; G3PDH – glyceraldehyde 3 phosphate dehydrogenase; DiI,1,1′-dioctadecyl-3,3,3′,3′-tetramethyl-indocarbocyanine-perchlorate

Introduction

Control of the multi-step metastatic cascade involves an interplay between many genes. Metastasis-regulatory genes can be classified as metastasis-promoting (i.e., driving conversion from non-metastatic to metastatic) and metastasis-suppressing. Metastasis suppressor genes, although akin to tumor suppressors, are distinct in that they block the spread of the tumor cells, without affecting primary tumor formation [1]. A tumor suppressor, on the other hand, also blocks metastasis since tumorigenicity is a prerequisite to metastasis. Interestingly, while metastasis requires coordinated expression of many genes, it takes only one gene to inhibit metastasis at any step of the cascade [2]. To date, only eight metastasis suppressor genes (*NME1* [3], *KiSS1* [4–6], *KAI1* [7], *CAD1* [8, 9], *MKK4* [10], Maspin [11, 12], TIMPs [13, 14], BRMS1 [15]) have been shown to suppress human cancer metastasis using *in vivo* models [reviewed in [2, 16]].

Of those genes, the mechanisms of action are generally not known. The current experiments were designed to begin elucidating the mechanism(s) of action of BRMS1, a metastasis suppressor recently discovered by us. Briefly, BRMS1 was isolated from metastasis-suppressed microcell hybrids of full-length human chromosome 11 and the human breast carcinoma cell line MDA-MB-435 by differential display

Correspondence to: D.R. Welch, Jake Gittlen Cancer Research Institute, Mailstop H059, The Pennsylvania State University College of Medicine, 500, University Drive, Hershey, PA 17033-2390, USA. Tel: +1-717-531-5633; Fax: +1-717-531-5634; E-mail: drw9@psu.edu

[15]. Transfection of full-length BRMS1 cDNA into MDA-MB-435 and MDA-MB-231 suppressed metastasis formation without affecting tumorigenicity, meeting the functional definition of metastasis suppression described above. That the BRMS1 gene maps to 11q13.1 to 11q13.2, a region frequently altered in late-stage breast carcinoma [2], provides further impetus to determine the mechanism by which this candidate metastasis suppressor functions. However, the mechanism by which BRMS1 would suppress metastasis is not obvious based upon the predicted amino acid sequence [15]. The BRMS1 protein is predominantly nuclear, contains imperfect leucine zipper and coiled-coil domains and a large glutamic acid rich region at the N-terminus. While mutational analysis is ongoing, a functional approach was undertaken in this study.

Materials and methods

Cell lines

MDA-MB-435 and MDA-MB-231 are human estrogen- and progesterone receptor- negative cell lines derived from metastatic infiltrating ductal breast carcinomas [17]. Both cell lines form progressively growing tumors when injected into the mammary fat pads of immunocompromised mice. MDA-MB-435 cells develop macroscopic metastasis in lungs and regional lymph nodes 10–12 weeks after inoculation, but rarely metastasize following direct injection into lateral tail vein. The opposite pattern of metastasis formation exists for MDA-MB-231 in athymic mice. So, for the latter, only intravenous inoculations were used to assess metastatic (colonization) potential.

BRMS1 transfectants were derived following transfection of full-length *BRMS1* cDNA (see below) cloned into the constitutive mammalian expression vector, pcDNA3 (Invitrogen, San Diego, California). All the cell lines were cultured in a 1:1 mixture of Dulbecco's-modified minimum essential medium and Ham's F-12 medium (DME-F12), supplemented with 5% fetal bovine serum (FBS; Atlanta Biologicals, Atlanta, Georgia), 1% non-essential amino acids, 1.0 mM sodium pyruvate, but no antibiotics or antimycotics. Transfected cells also received 500 μg/ml G-418 (Life Technologies, Inc., Gaithersburg, Maryland).

All cell cultures were maintained on 100 mm Corning tissue culture dishes, at 37 °C, with 5% CO_2 in a humidified atmosphere. When cultures reached 80–90% confluence, they were passaged using a solution of 0.125% trypsin, 2 mM EDTA (TE) in Ca^{+2}/Mg^{+2}-free Dulbecco's phosphate buffer saline (CMF-DPBS). BRMS1-transfected 435 cells acquired an unexplained acute sensitivity to trypsin; so cultures were passaged thereafter using 2mM EDTA solution in CMF-DPBS. Cells could be routinely split at ratios of 1:10–1:30. *In vitro* doubling times for all cells were between 24–36 h. MDA-MB-435 and MDA-MB-231 were used between passages 119–139 and 161–166, respectively. Hybrid clones and transfectants were used before passage 11 in order to minimize the impacts of clonal diversification and phenotypic instability [18]. For all functional and biological assays, cells between 70–90% confluence were used, with viability >95%. All the lines were routinely checked and found negative for *Mycoplasma* spp. contamination using the GenProbe method (Fisher Scientific, Pittsburgh, Pennsylvania).

Cell line nomenclature was developed to identify the origin and nature of each cell line as unambiguously as possible. Single-cell clones are identified by parental cell line name preceding a '.' followed by clonal designation. Uncloned populations are identified by a '-' after the parental cell line name. Where appropriate, numbers in parentheses following the cell line designation indicate the number of subcultures following cloning or establishment of the cell line. Numbers preceded by 'TE' indicate that cells were passaged in a mixture of trypsin-EDTA. Numbers preceded by a 'P' indicate the cells passed using EDTA alone.

Transfection

BRMS1 was cloned into the constitutive mammalian expression vector pcDNA3 (Invitrogen, San Diego, California) under control of the cytomegalovirus promoter. To detect BRMS1 protein expression, a chimeric molecule was also constructed with an N-terminal epitope tag (SV40T epitope 901 [19, 20]). Epitope-tagged and native *BRMS1* plasmids as well as pcDNA3 vector only were transfected into MDA-MB-435 and MDA-MB-231 cells by electroporation (BioRad Model GenePulser™, Hercules, California; 220V, 960 μFd, $\infty\Omega$). Briefly, cells (0.8 ml; 1×10^7 cells/ml) from 80% confluent plates were detached using 2 mM EDTA solution. Plasmid DNA (10–40 μg) was added to the cells and the mixture placed onto ice for 5 min before electroporation, followed by 10 min on ice prior to plating onto 100 mm tissue culture dishes. One day later, transfectants were selected by addition of G-418. Single cell clones were isolated by limiting dilution in 96-well plates and confirmed visually to originate from single cells. Stable transfectants of *BRMS1* were assessed for their expression of transcripts by northern blotting and/or immunoblotting.

Northern blot hybridization

Poly(A)$^+$-enriched mRNAs (2 μg) or total RNA (20 μg) were size separated on 1% agarose formaldehyde gels before transferring onto a positively charged Hybond-N$^+$ nylon membrane (Amersham Pharmacia Biotech., Arlington Heights, Illinois) using the Turboblotter system (Schleicher & Schuell, Keene, New Hampshire) and fixed by UV cross linking. All prehybridizations and hybridizations were carried out using ExpressHyb solution (Clontech, Palo Alto, California) according to manufacturer's recommendations, except that washes were done at 55 °C rather than 50 °C. The membranes were exposed to Kodak BioMAx MR X-ray film. Equal loading and transfer efficiency were assessed by hybridizing the blots with human G3PDH cDNA (Pst1/Kpn1 780 bp fragment ATCC57090/ATCC57091 in pBR322).

The expression of *BRMS1* mRNA in multiple human tissues was done using a human mRNA multiple tissue north-

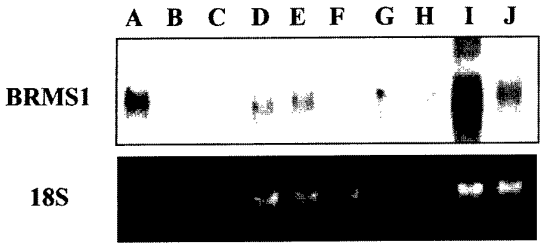

Figure 1. Variable expression of BRMS1 by breast carcinoma cell lines. Equal amounts (10 μg) of total RNA were loaded in each lane. Full-length BRMS1 cDNA isolated from adult human kidney library in λTripIEx was used as probe. Intensity of ethidium bromide stained 18S RNA bands was used as a loading control. Lanes: A, neo11/435 (positive control); B, blank; C, MDA-MB-435; D, MDA-MB-231; E, LCC15; F, SUM185; G, MCF7; H, MCF10AT; I, MKL4; J, T47D^{CO}.

ern blot (Clontech). For measuring expression of BRMS1 in human breast carcinoma cell lines with varying malignant properties, total RNA was isolated from 80% confluent monolayer cultures using TRIzol (Life Technologies Inc.) according to the manufacturer's instructions.

Southern blot hybridization

The presence of a *BRMS1* gene homolog in various eukaryotic species other than human was examined by Southern blot hybridization. Full-length *BRMS1* cDNA was used to probe a zoo-blot (Clontech) that had genomic DNA from nine eukaryotic species (chicken, cow, dog, human, monkey, mouse, rabbit, rat, yeast) digested with EcoRI, resolved on a 0.7% agarose gel, transferred to a charge modified nylon membrane by capillary transfer and fixed by UV irradiation.

Immunoblotting

A monoclonal antibody developed against amino acids 684–698 of the SV40T antigen (designated 901 epitope) was generously provided by Dr Satvir Tevethia, Department of Microbiology and Immunology, Penn State University College of Medicine. *BRMS1* with 901 epitope, fused inframe to the N-terminus was cloned into pcDNA3 before transfection and sequence verified. BRMS1 expression was determined by collecting total protein of 70–90% confluent cell cultures. Following aspiration of medium, plates were rinsed 3× with CMF-DPBS before addition of 1 ml lysis buffer (50 mM Tris-HCl, pH 6.8; 2% β-mercaptoethanol, 2% SDS). Lysates were centrifuged at 10, 000 × g at 4 °C for 15 min to remove insoluble material. Protein concentration was determined using the Bradford method. Protein (20–30 μg/lane) was mixed with 5× loading buffer (50% glycerol, 1.5% bromophenol blue) and separated by 12.5% SDS-PAGE. Protein was transferred to Poly Screen® membrane (NEN-Dupont) by semi-dry transfer (5.5 mA/cm^2, 20 V, 30 min). Proteins were fixed by air drying for 15 min at room temperature. The membrane was then wetted in methanol, rinsed in distilled water and blocked in a TTBS solution (0.05% Tween-20, 20 mM Tris, 140 mM NaCl, pH 7.6) containing 5% dry non-fat milk for 1 h. The 901-tagged BRMS1 was detected using 1:5000 dilution of mouse anti-901 ascites for 1 h at room temperature under constant agitation. Membranes were then washed with TTBS and probed with 1:10,000 dilution of sheep anti-mouse secondary antibody conjugated to horseradish peroxidase (Amersham-Pharmacia Biotech, Buckinghamshire, UK) in a solution of 5% nonfat dry milk/TTBS for 1 h at room temperature before washing in TTBS. Bound secondary antibodies were detected using ECL™ (Amersham-Pharmacia Biotech) for 30 sec to 10 min Similar protocols were used to detect Kai1 (rabbit anti-Kai1, Santa Cruz; 1:5000); Nm23 (rabbit anti-human Nm23, NeoMarker, Fremont, California, 1:5000) and E-cadherin (rabbit anti-E-cadherin, Transduction Laboratories, Lexington, Kentucky, 1:3000) using donkey anti-rabbit IgG HRP conjugate as a secondary antibody at a titer of 1:5000. Some of the blots were re-probed after being stripped using a solution of 200 mM glycine, 50 mM potassium acetate and 0.2%-mercaptoethanol, pH 4.5.

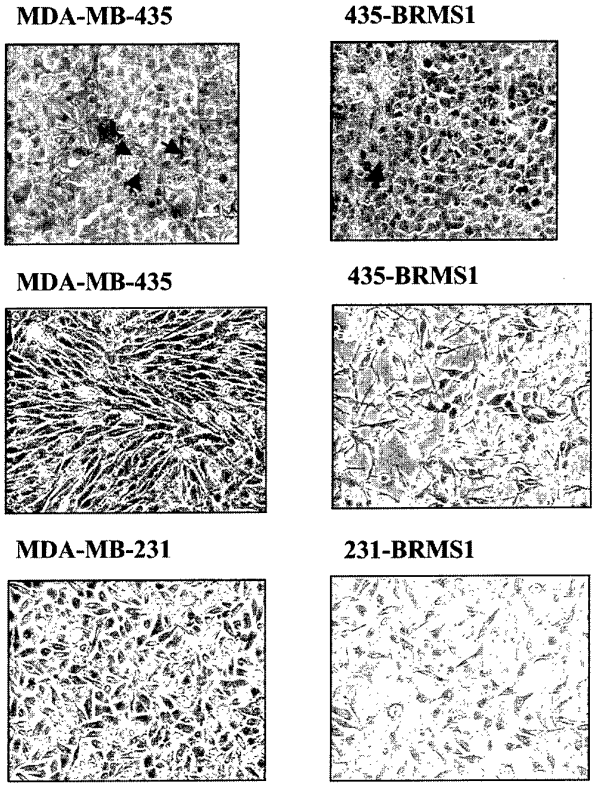

Figure 2. Histology (top row) of BRMS1-transfected MDA-MB-435 tumors revealed poorly differentiated, locally invasive masses. Cells (1×10^6) were injected into the mammary fat pads of athymic mice. Tumors were removed approximately 4 weeks after injection, fixed in formalin, sectioned and stained with hematoxylin and eosin. The tumor formed by MDA-MB-435 cells (magnification ~160×) exhibited tightly packed cells with polymorphic nuclei and prominent nucleoli. Fibrous bands (arrows) are present throughout the tumor. Tumors formed by BRMS1 transfectants (magnification ~160×) were histologically similar with tightly packed cells, nuclear degeneration and occasional mitotic figures (arrow heads). Stromal elements of these two tumors were somewhat different (i.e., BRMS1 exhibited fewer fibrous bands). *In vitro* morphologies of BRMS1-transfected MDA-MB-435 or MDA-MB 231 did not show consistent major alterations in morphology compared to vector-only transfectants.

Metastasis assays

Immediately prior to the injection, cells (7-11 passages following transfection) at 80–90% confluence were detached with 2mM EDTA solution, washed with CMF-DPBS, counted using a hemacytometer and resuspended in ice-cold HBSS to a final concentration of 2.5×10^6 cells/ml for MDA-MB-231 and 10^7 cells/ml for MDA-MB-435. Eight mice per experimental group were used and each experiment was performed at least two times independently.

MDA-MB-231 cells and derivatives (2×10^5 in 0.2 ml) were injected into the lateral tail vein of 3–4 weeks old, female athymic mice (Harlan Sprague-Dawley, Indianapolis, Indiana) using a 27 gg needle affixed to a 1 cc tuberculin syringe. Mice were killed 4 weeks post-injection and examined for the presence of metastasis. Lungs were removed, rinsed in water and fixed in diluted Bouin's solution (20% Bouin's fixative in neutral buffered formalin) before quantification of surface metastasis as previously described [21].

Similar procedures were used for the spontaneous metastasis assays using 435 cell, except that 1×10^6 cells (0.1 ml) were injected into exposed axillary mammary fat pads of anaesthetized (Ketamine 80 mg/kg, Xylazine 14 mg/kg) 5–6 weeks old, female athymic mice. Some tissue from local tumors and metastatic lesions was preserved in neutral-buffered formalin or diluted Bouin's fixative for histologic analysis to verify gross observations. Sections (4–6 μm thick) were prepared by dehydration, paraffin embedding, sectioning and staining with hematoxylin and eosin.

Tumor size was measured weekly by taking perpendicular measurements and was expressed as mean tumor diameter. Mean tumor diameter was calculated as described by use of the following equation: $\sqrt{(\text{diameter}_x)(\text{diameter}_y)}$, where x is the largest diameter of the locally growing tumor.

After the mean tumor diameter reached 1.5–2.0 cm, tumors were surgically removed under Ketamine: Xylazine (80–85 mg/kg: 14–16 mg/kg) anesthesia and the wounds closed with sterile stainless steel clips (9 mm). Four weeks later, mice were killed and visible metastasis were counted. Metastases were observed in ipsilateral and contralateral axillary lymph nodes and lungs of control mice. Occasional recurrence developed at the site of tumor removal but the presence of hematogenous metastasis did not necessarily correlate with the presence of recurrent tumor.

Surface lung metastases were counted as described [21]. Briefly, pale yellow raised masses (typically >0.25 mm) were observed on more darkly staining lungs. The size of lung metastases ranged from ~0.25 mm to 1.0 mm. Microscopic lesions were occasionally observed in histologic sections. Axillary lymph nodal metastases were scored as present or absent.

Animals were maintained under the guidelines of the National Institute of Health and the Pennsylvania State University College of Medicine. All protocols were approved by Institutional Animal Care and Use Committee. Food and water were provided *ad libitum*.

Growth in soft agar

Cells (1×10^3) suspended in 0.35% agar (Fisher Scientific) were plated onto a layer of 0.75% Bacto agar in DME-F12 + fetal bovine serum (5%) in 6-well tissue culture dishes. The agar containing cells was allowed to solidify overnight in a CO_2-containing humidified incubator. Additional DME-F12 + fetal bovine serum (0.5 ml) was overlaid onto the agar and the cells were allowed to grow undisturbed for 14–15 days. Visible colonies (>50 cells) were counted with the aid of a dissecting microscope.

Adhesion assays

Single cell suspensions of breast cancer cells in pre-warmed DME-F12 containing 5% FBS (8×10^5 cells/ml, 250 μl/well) were plated onto each well of extracellular matrix-coated plates and incubated for 1 h at 37 °C. The media were aspirated and each well was washed with pre-warmed Dulbecco's PBS to remove unbound or weakly bound cells. After fixation with 2% formaldehyde for 10 min, the adhering cells were stained with 0.1% crystal violet, rinsed with water, and air dried. Dye was extracted in a mixture of water:ethanol:methanol (5:4:1; v:v:v) and absorbance was measured at 590 nm in a spectrophotometer (Beckman, DU650, Fullerton, California).

Motility assay

A Boyden chamber assay was used with minor modification. Briefly, lower chambers were filled with 0.9 ml 5% FBS-supplemented DME-F12 before the chambers were assembled. Sterile 8-mm polyethylene terepthalate filters (Collaborative Biomedical Products, Cat. No. 354578, Bedford, Massachusetts) were placed in the chambers and 0.25 ml 5% FBS-supplemented DME-F12 containing 5×10^4 tumor cells was placed into the upper chambers and incubated at 37 °C in 5% CO_2 humidified atmosphere for 18 h. The filters were then removed and membranes were fixed in 2% paraformaldehyde and stained with 1% crystal violet. Cells on the upper side of the filter were removed with a cotton swab and the motile cells which had migrated to the lower side of the filter were counted under microscope. Each test group was assayed in triplicate. Six random microscope fields (magnification 200×) were counted in each replicate well and results were expressed as cells per high power field.

Wound motility assay

Cells were cultured to confluence on 6-well plates (50,000 cells/well, initial plating) and subsequently a central, linear scrape wound was made with a sterile blue tip. Phase micrographs of the wound cultures were taken at 0 and 18 h (to minimize the effect of cell doubling, average doubling time is ~24 h). The photographs were analyzed by measuring the distance from the wound edge of the cell sheet to the original wound site. Migration activity was calculated as the mean distance between edges in 15 fields per well. Each test group was assayed in triplicate, and results were expressed relative to parental cell migration.

Gap junctional communication assay

To assay homotypic gap junctional intracellular communication, MDA-MB-231, vector only transfectants and BRMS1 transfectant clone 13 were examined using a double labeling fluorescence dye transfer technique.

'Acceptor' cells were plated onto a glass coverslip and grown to near confluence. Following twice washing with buffered saline, the 'Donor' cells were labeled with a PBS-fluorescent dye mixture containing 20 μl calcein AM (Molecular Probes, Eugene, Oregon) and 7 μl DiI (Molecular Probes) 2 ml bovine serum albumin (20 mg/ml) and 20 μl pluronic acid (Molecular Probes) and incubated for 30 min at 30 °C. Calcein can be transferred through gap junctions while DiI cannot. The later serves as a marker for the donor cells when calcein levels have been lowered below the level of unambiguous detection. 'Donor' cells were then washed, detached and dropped onto a monolayer of the 'Acceptor' cells at a ratio of ~ 1:500. Following a 90 min incubation at 37 °C, green dye transfer to the accepting cells was visualized using fluorescence (λ_{ex} = 450–490 nm; λ_{em} = 520 nm) and rhodamine (λ_{ex} = 546 nm; λ_{em} = 590 nm) filters. Donor cells appeared yellow or red while acceptor cells were green (if dye transfer occurred) or colorless (if gap junctional intracellular communication was not functional). A limited number of corroborating experiments were done using direct injection and the conclusions were identical (data not shown).

RT-PCR analysis

To test the heparanase expression, total RNA was isolated from MDA-MB-435 and MDA-MB-231, and various BRMS1 transfectant clones using TRIzol reagent. Total RNA (2.5 μg) was used a a template for RT-PCR using Advantage One-Step RT-PCR kit (Clontech). Human G3PDH was amplified as a control with purchased primers (Clontech) with an expected product size of 983 bp. Heparanase RNA was amplified using the primers HPA-F (5′-TTCGATCCCAAGAAGGAATCAAC-3′) and HPA-R (5′-GTAGTGATGGCCATGTAACTGAATC-3′) at 100 moles with an expected size of 585 bp. Reverse transcription was done at 50 °C for 60 min. Samples were then denatured at 94 °C for 5 min, followed by 35 cycles of PCR (94 °C – 45 s; 60 °C – 45 s; 72 °C – 1 min) and a final extension step (10 min at 72 °C). Product was subjected to electrophoresis on 2% agarose gel, stained with ethidium bromide and visualized under UV light.

Enzymography

Conditioned media from identically confluent culture were analyzed for MMP2 and MMP9 activity in gelatin impregnated SDS-poly acrylamide gel as described previously [22]. Briefly cell-free media were collected from 80% confluent plates and resolved on 8% SDS-PAGE (containing gelatin (1 mg/ml) EIA grade [Bio-Rad]), prior to reduction or heat denaturation. After electrophoresis, the gels were washed in several volumes of de-ionized water (without harsh agitation) and then incubated at 37 °C, overnight in digestion buffer (10 mM $CaCl_2$, 50 mM Tris pH 7.2 and 500 mM NaCl). The gel was then stained with Coomassie Brilliant Blue R-250 (Bio-RAD). Pre-stained SDS-PAGE protein standards (Rainbow Markers, Amersham) were used for estimating molecular weight.

$^{32}P_i$ labeling of BRMS1

Since computer models predicted presence of several consensus phosphorylation sites in BRMS1 protein [15], a crude measurement of phosphorylation was done. BRMS1-expressing cells were grown to 80% confluence, washed and placed into phosphate free medium. $^{32}P_i$-ortho-phosphate pulse was then given for 3 h. The medium was aspirated and cells were lysed under non-denaturating conditions. 901-tagged BRMS1 was immunoprecipitated and subjected to SDS-PAGE and transferred to a PVDF membrane. Following localization of BRMS1 by immunoblotting with anti 901 antibody, the membrane was then subjected to fluorography for the detection of incorporated radiolabeled phosphate.

Subcellular fractionation for isolation of nuclear and cytoplasmic fractions

MDA-MB-435.BRMS1.3 cells grown to 80% confluence were used for fractionation. The growth medium was aspirated; the plate was rinsed 2× with 5 ml ice-cold CMF-PBS and cells removed with a teflon-coated scraper (Costar). Cells were centrifuged at 500 *g* for 5 min at 4 °C and supernatant was discarded. The cell pellet was loosened by gently vortexing for 5 s followed by addition of 4 ml Nonidet P-40 (NP-40) lysis buffer (10 mM Tris HCl, pH 7.4, 10 mM NaCl, 3 mM $MgCl_2$, 0.5% v/v NP-40) with continuous vortexing to minimize clumping and uniformly resuspend cells. After incubation for 5 min on ice, an aliquot was examined under a phase contrast microscope to ensure that cells had uniformly lysed and the nuclei were free of cytoplasmic material. The supernatant was aspirated after spinning for 5 min at 500 × *g* at 4 °C. The nuclear pellet was suspended in 4 ml NP-40 lysis buffer with simultaneous vortexing and centrifuged for 5 min at 500 × *g* at 4 °C. The pellet was then suspended in 200 μl glycerol storage buffer (50 mM Tris Cl, pH 8.3, 40% v/v glycerol, 5 mM $MgCl_2$, 0.1 mM EDTA) by gentle vortexing. BRMS1 was detected by anti-901 antibody and lamin A/C (Antibody 636; SC-7292; Santa Cruz Biotechnology)was used as a positive control [23]. Similar results were obtained using equal protein or cell-equivalent loading parameters.

Immunofluorescence

To detect the subcellular localization of BRMS1, cells were grown to to 60–80% confluence. Medium was removed by aspiration and washed 3× with chilled CMF-PBS. Cells were fixed in 2% paraformaldehyde (pH 7.0) on ice for 30 min before rinsing 3× with chilled CMF-DPBS. Cells and nuclei were then permeabilized and stained with 0.1% Triton X100 containing 0.1 mg DAPI (Sigma) in CMF-

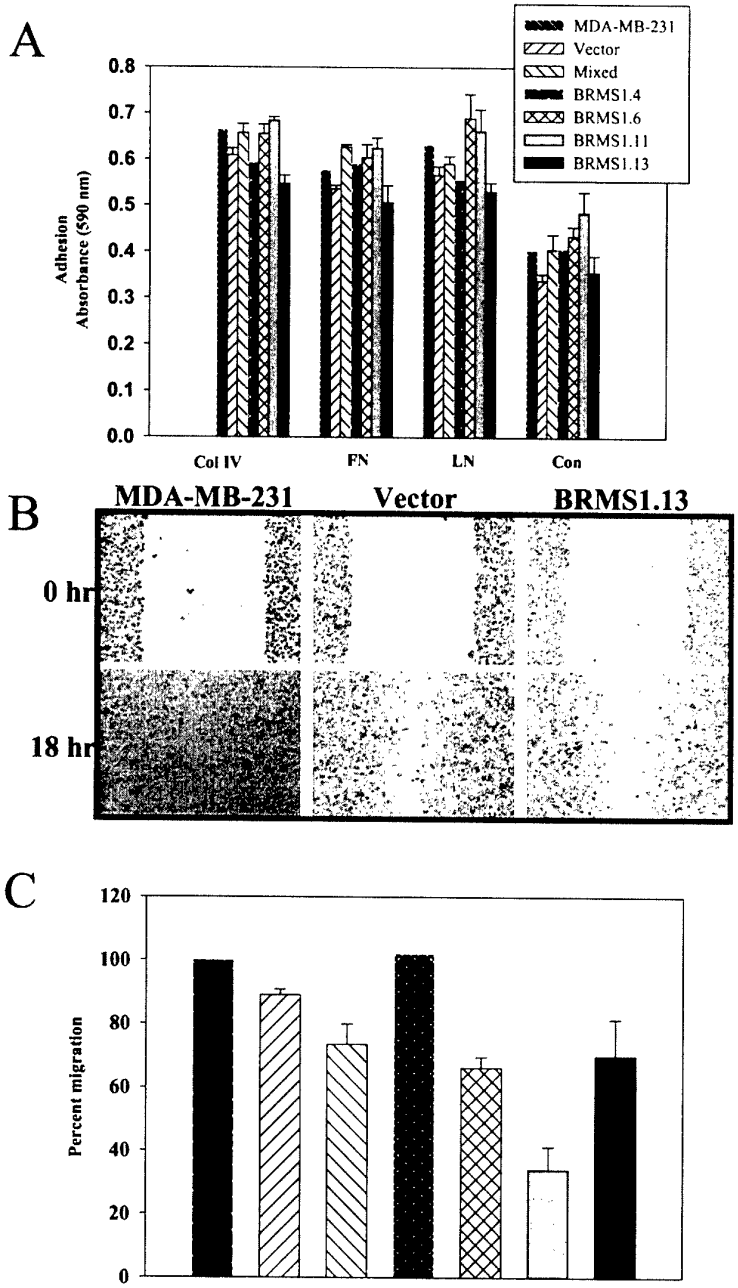

Figure 3. Adhesion (panel A) of MDA-MB-231 and BRMS1 transfectants to extracellular matrix components (type IV collagen (Col IV), fibronectin (FN), laminin (LN)) and cell culture plastic (Con) is not altered significantly for MDA-MB-231 BRMS1 clones. Adherent cells were quantified by staining with 0.1% crystal violet and absorbance at 590 nm after 1 h at 37 °C. Results represent mean ± standard deviation ($n = 3$) in a representative experiment. B. Motility as measured by the ability of human breast carcinoma cells to migrate into a wound created on a cell monolayer. Representative photographs of wound healing assay for MDA-MB-231, MDA-MB- 231.pCDNA3(vector), MDA-MB-231.BRMS1.13. C. Comparative motility from the wound healing assay is depicted as percent migration of the wild type. The legends for panels A and C are identical. Relative BRMS1 protein expression in individual clones is found in Figure 6.

DPBS for 3–5 min and washed 5× with chilled CMF-PBS. Subsequently cells were stained with primary antibody (anti-901(1:1000) in CMF-DPBS) and visualized with fluorescein-conjugated goat anti-mouse secondary antibody (Organon Teknika, Research Triangle Park, North Carolina (1:250)). Staining of the parental cells with primary antibody (anti-901) as a negative control showed no staining.

Results and discussion

BRMS1 expression

BRMS1 cDNA was originally isolated from a human kidney cDNA library for technical reasons but expression is widespread, including in normal breast tissue, [15] (data not shown). Transcript size was approximately 1.5 kb and

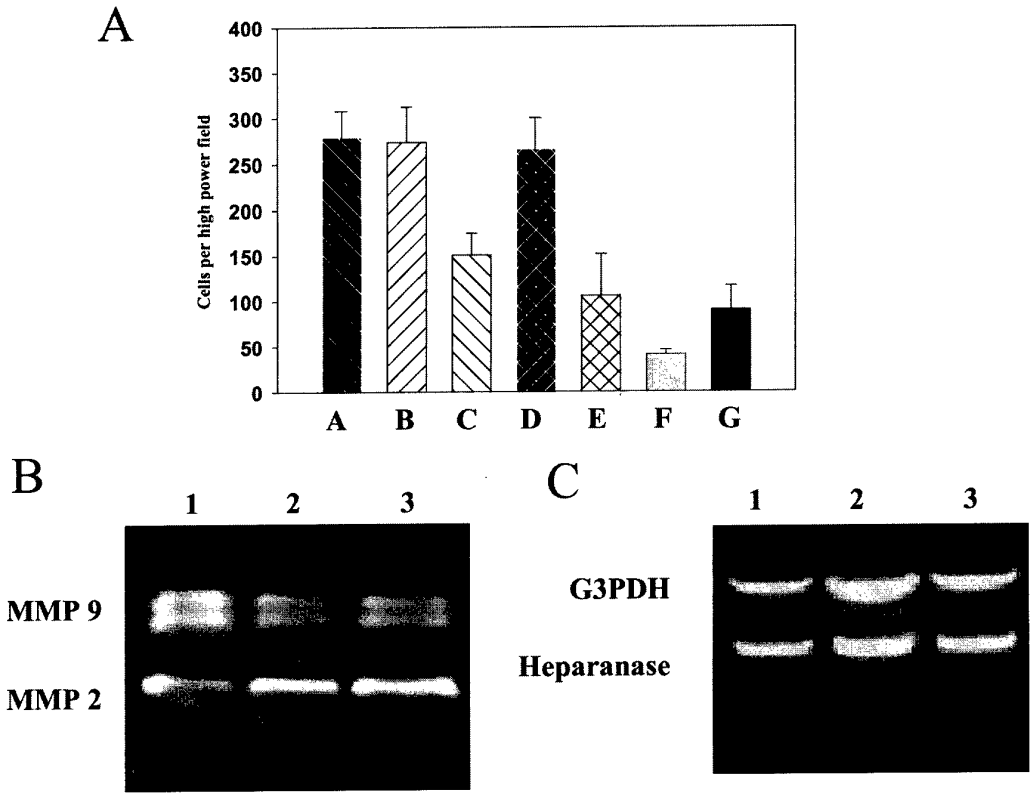

Figure 4. A. Invasion through a Matrigel-coated filter is partially suppressed in BRMS1-transfectant human breast carcinoma cells. MDA-MB-231 (A), MDA-MB-231-pcDNA3 (vector) (B), mixed pool of BRMS1 transfectants without tag (C) and MDA-MB-231.BRMS1 clones [(D) BRMS1.4; (E) BRMS1.6; (F) BRMS1.11; (G) BRMS1.13] with varying levels of BRMS1 expression (see Figure 6) were measured for their ability to transverse a filter in a modified Boyden chamber apparatus within 18 h. B. The production of matrix metalloproteinases was studied by gelatin impregnated SDS-PAGE enzymography. Cells (0.5×10^6) were seeded onto a fresh tissue culture plate and cell free media was collected from 80% confluent plates. Proteins were resolved on 8% SDS-PAGE (containing gelatin (1 mg/ml)) prior to reduction or heat denaturation. After electrophoresis, the gels were washed then incubated at 37 °C in digestion buffer, stained with Coomassie Brilliant Blue R-250. MDA-MB-231 (lane 1) , MBA-MB-231-pcDNA3 [vector control] (lane 2) , MDA-MB-231.BRMS1.13 (lane 3). C. Analysis of heparanase expression in BRMS1 transfectants. Total RNA (2.5 μg) was used as template for RT-PCR. G3PDH was amplified as an internal control with an expected product size of 983 bp. Heparanase was amplified with an expected size of 585 bp. Lane 1. MDA-MB-231, Lane 2. MDA-MB-231-pcDNA3, Lane3. MDA-MB-231.BRMS1.13. Note: Relative invasion in Figure 4 correlates well with motility in Figure 3. Also note that the suppression of motility and invasion is least in the lowest BRMS1-expressing clone (BRMS1.4).

an epitope-tagged protein migrates to Mr ~35 kDa (epitope size is ~1.3 kDa). There was no evidence for alternative splicing in any of the tissues, although expression levels varied considerably. To test the hypothesis that BRMS1 expression levels or mutations might correlate with aggressive behavior in human breast carcinoma cell lines, RNA blots were examined (Figure 1). MDA-MB-435 [17], SUM185 [24], MCF7 [25] and SV40T-transformed MCF10AT [26, 27] express *BRMS1* at a low level. MDA-MB-231 [17], LCC15 [28] and T47D^{Co} [29] express moderate levels of *BRMS1*. MKL4 (FGF4-transfected MCF7 cells [30]) expresses a relatively high level of BRMS1. These results clearly show quantitative differences in expression, but relationship to behavior is more complex. Except for MCF10AT, all of the other cell lines were derived from metastases, but in our laboratory, only MDA-MB-435, MDA-MB-231 and LCC15 metastasize in athymic mice. Although, *BRMS1* mRNA levels *per se* do not predict metastatic ability in athymic mice, there was no evidence for gross rearrangement, deletion or mutation. To rule out these possibilities conclusively, more extensive studies will be required and are underway.

BRMS1 orthologs, or partial orthologs, exist in a wide variety of species (mouse, rat, dog and cow) as seen in a zoo blot (data not shown). BLAST searches show ESTs with homology to Drosophila, pig and cow as well. Preliminary data with the recently cloned murine homolog (Samant et al., in press) shows greater than 85% homology at the nucleotide and >94% identity at the protein level.

Constitutive expression of *BRMS1* in MDA-MB-231 and MDA-MB-435 human breast carcinoma cells significantly reduced lung and lymph node metastasis (Table 1). Locally growing tumors still developed when 1×10^6 cells (of either cell line) were injected into the mammary fat pads of athymic mice. Histologic examination of locally growing tumors and metastases revealed poorly differentiated masses that were locally invasive. The only noteworthy difference between parental and BRMS1 transfectants was a decrease in stromal fibrous bands in the latter (Figure 2). *In vitro* morphologies were unremarkable (Figure 2), as were *in vivo* and *in vitro* growth rates and saturation densities [15]. Oc-

Table 1. BRMS1 suppresses human breast cancer metastasis.

Cell line	No. lung metastases (mean ± SEM)
MDA-MB-435 (vector control)[a]	40 ± 22
BMRS1.1	1 ± 0.6*
BRMS1.3	1.5 ± 1.3*
BRMS1.6	<1*
MDA-MB-231 (vector control)[b]	148 ± 20
BRMS1.4	88 ± 18
BRMS1.6	46 ± 11*
BRMS1.11	28 ± 7*
BRMS1.13	18 ± 6*
BRMS1 (mixed pool)	22 ± 10*

[a]Cells (1×10^6) were injected into the mammary fat pads of 4–6-week-old female athymic mice. When tumors reached a mean tumor diameter of 1.2–1.5 cm, they were removed. Mice were killed 4 weeks after tumor removal and presence of metastases determined.
[b]Cells (2×10^5) were injected intravenously into 3–4-week-old female athymic mice. Mice were killed 5 weeks after injection and the number of lung metastases quantified.
*Significantly different from control ($P < 0.05$).
The incidence of axillary lymph node metastasis was also reduced in BRMS1 transfectants (data not shown).

casional microscopic lung lesions were observed; however, only macroscopic metastases are quantified.

Steps in metastasis affected by BRMS1 expression

The ability to suppress metastasis without inhibiting tumorigenicity satisfies our definition of a metastasis suppressor. So, studies were done to explore the step(s) in metastasis altered by BRMS1 expression.

Unexpectedly, *BRMS1*-transfected MDA-MB-435, but not MDA-MB-231, acquired acute sensitivity to trypsin. Although an explanation has not been determined, this finding required modification of cell culture protocols (i.e., use of EDTA only rather than a trypsin-EDTA mixture). Moreover, the result suggested that the cell surface was different, implying that corresponding phenotypes (e.g., adhesion) might also be affected by BRMS1. To test this, cell adhesion to extracellular matrix components type-IV collagen, fibronectin and laminin were measured. Representative results are shown in Figure 3A for MDA-MB-231 although results are similar for transfectant of MDA-MB-435. Although the highest BRMS1 expressing clone, MDA-MB-231.BRMS1.cl.13, showed consistently lower adhesion than other clones, differential adhesion is not thought to be a major consequence of BRMS1 overexpression since metastasis by the other clones was also suppressed despite no or modest diminishment of adhesion.

That the locally growing tumors were still invasive suggested that BRMS1 was not acting through this step in the metastatic cascade. However, the *in vivo* measures of invasion are not readily quantified. Thus, the ability to invade through a Matrigel-coated polycarbonate filter *in vitro* was assessed as was expression of heparanase and MMP2 and MMP9. Representative results are shown for MDA-MB-231 transfectants (Figure 4A). BRMS1 transfectants were generally less invasive, but inhibition did not correlate with BRMS1 expression. Semi-quantitative RT-PCR analysis of heparanase levels or MMP2 and MMP9 activity by enzymography revealed no consistent differences in the production of these proteinases either (Figures 4B and 4C).

Lowered invasion in the absence of apparent reductions in proteinase expression and/or activity suggested that BRMS1 might decrease cellular motility, a key component of invasion. Two assays were employed to test this hypothesis – a modified Boyden chamber assay [31] and a monolayer wound healing assay [32] (Figures 3B and 3C). Both methods showed modest, (30–60%), but significant reduction in motility in BRMS1 transfectant MDA-MB-231 and MDA-MB-435 cells compared to parent or vector control.

The above results are relatively predictable in that motility and invasion are well-established, necessary steps in the metastatic cascade [33–36]. However, the level of suppression of motility and invasion are modest in comparison to the degree of metastasis suppression observed in *BRMS1* transfectants. While not discounting these findings, other mechanisms were also suspected to be involved.

Several laboratories have explored correlations between ability of tumor cells to grow in soft agar and metastatic potential [37–40]. Therefore, we tested the anchorage-independent growth efficiency of BRMS1 transfectants. Colony formation was significantly less in MDA-MB-435 transfectants. Parental MDA-MB-435 cells formed 135 ± 8 colonies compared to BRMS1-transfectant clones 3 and 6 (15 ± 5 and 28 ± 8, respectively). However, the effect of BRMS1 on MDA-MB-231 was more modest. Parental cells formed 152 ± 10 colonies compared to BRMS1-transfectant clones 4, 6, 11 and 13 (168 ± 7; 145 ± 12; 130 ± 15 and 133 ± 8, respectively). MDA-MB-231BRMS1cl.4 is non-expressing; whereas, the other clones express variable levels of protein. Therefore, differences in anchorage-independent growth cannot explain metastasis suppression in the human breast carcinoma cell lines.

A growing body of data demonstrating reduction in gap junctional intercellular communication with transformation [41, 42] and progression towards metastasis [43–45] has developed over the past quarter century. Gap junctions are intercellular channels allowing exchange of small (<1 kDa) molecules between juxtaposed cells [46]. Nicolson and colleagues showed that gap junction function decreased with increasing metastatic potential among a series of rat mammary adenocarcinomas [45]. Gap junction function was tested in BRMS1-transfected MDA-MB-231 cells and corresponding parental and vector only transfectants (Figure 5A). The results show clearly that BRMS1 expression restores homotypic gap junctional intercellular communication. Similar findings were observed in MDA-MB-435 cells [47].

The gap junction findings are perplexing in that the anticipated protein structure of BRMS1 would not predict it to function at the cell surface in this manner. The BRMS1 cDNA and genomic sequences are predicted to encode a novel protein of 246 amino acids (28.5 kDa). Although several putative consensus phosphorylation sites are present in the sequence, $^{32}P_i$ labeling has never revealed a phos-

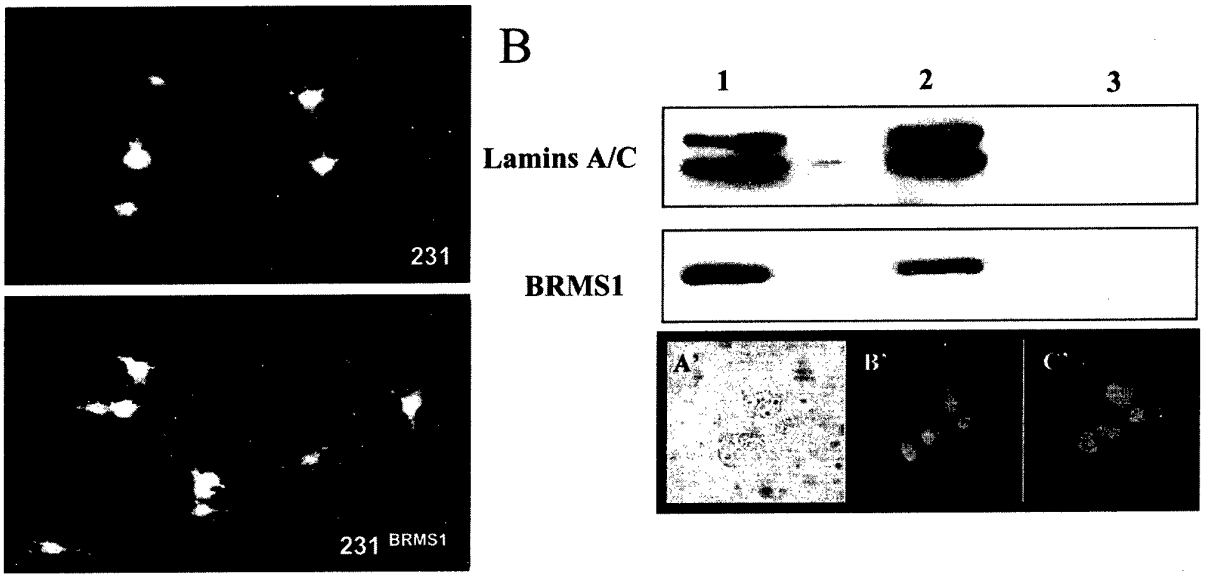

Figure 5. BRMS1 is predominantly a nuclear protein which restores homotypic gap junctional intercellular communication. A. BRMS1 restores GJIC in MDA-MB-231 cells. Calcein-loaded MDA-MB-231 cells or MDA-MB-231.BRMS1.13 were placed into contact with a monolayer of like cells (e.g., MDA-MB-231 on MDA-MB-231 monolayer). Dye remained in MDA-MB-231 cells; whereas, BRMS1 transfectants transferred dye to the recipient cells (magnification ~400×). Dye transfer was not observed with MDA-MB-231 cells in heterotypic GJIC assays (data not shown). B. BRMS1 is a nuclear protein. Western blots of cytosolic and nuclear fractions of 901-tagged BRMS1-transfected MDA-MB-435 cells. Anti-901 and anti-lamin antibodies (positive control) were used to detect nuclear proteins. Protein (4.2×10^5 cell equivalents per lane) was loaded. Lanes: whole cell lysate (1), cytoplasmic (2) and nuclear (3)] fractions were compared. Similar results were obtained in MDA-MB-231 cell variants (data not shown). Micrographs of phase contrast (A') and immunofluorescence (B' and C') confirm nuclear localization in MDA-MB-231 and MDA-MB-435 (not shown) cell variants. B' shows DAPI staining (positive control) while C' shows BRMS1 localization. BRMS1 was detected using anti-901 primary antibody and fluorescein-tagged goat-anti-mouse secondary antibody. Secondary antibody alone and vector-only transfectants did not exhibit nuclear staining (data not shown).

phorylated BRMS1 by immunoblotting or immunoprecipitation studies (data not shown). Briefly, an epitope-tagged BRMS1-construct [15] was transfected into MDA-MB-231 and a high expressing clone was cultured in phosphate free media supplemented with $^{32}P_i$. BRMS1 was immunoprecipitated using anti-901 antibody and was resolved by a SDS-PAGE. The gel was electro-blotted onto a PVDF membrane and fluorography did not reveal any $^{32}P_i$ labeled bands corresponding to BRMS1. The blot was simultaneously analyzed using ECL chemiluminescence for the immunoprecipitation.

The predicted BRMS1 protein sequence also shows two putative nuclear localization sequences at amino acids 198–205 and 239–245 [15]. Two complementary approaches were used to determine whether this sequence was functional. Nuclear protein extracted from 901-tagged BRMS1-expressing MDA MB 435 was immunoblotted and compared to cytosolic proteins from equivalent amounts of the same cells. BRMS1 was found predominantly in the nuclear fraction (Figure 5B). These results were corroborated by immunofluorescence studies using the anti-901 antibody as a primary antibody and RAM-FITC labeled secondary antibody. The BRMS1 fluorescence signal co-localized with a DAPI nuclear stain (Figure 5B). These results provide compelling evidence that BRMS1 is a nuclear protein.

Based on the nuclear localization and presence of other motifs indicative of roles in transcription complexes (e.g., leucine zippers, glutamic acid-rich region, coiled-coil domains), it was predicted that BRMS1 might regulate the expression of other metastasis suppressors. Although this was not directly tested, Western blot and Northern blot studies showed no correlation between BRMS1 expression and Kai1, Nm23, KiSS1 or E-cadherin expression (Figure 6). Preliminary studies suggest that BRMS1 may modulate expression of some gap junction components (Saunders et al., manuscript submitted), but more extensive studies are needed.

Collectively, these data extends the evidence that BRMS1 is a functional human breast cancer metastasis suppressor gene. The data also suggest that BRMS1 is operating by both conventional (i.e., invasion and adhesion) and unexpected means (i.e., GJIC) to inhibit metastasis. Based upon the presence of invasive cords in the locally growing tumor, BRMS1 appears to function downstream of the local invasion step. This is consistent with our findings of modest or no changes in invasion-related phenotypes, such as adhesion, MMP production and activity, heparanase production and motility. Although these results show reduced suppression of motility and invasion, it is important to emphasize that maximal abilities are not essential for metastases to form. Cells must only be adequate or competent in those abilities [48, 49].

The more intriguing finding is that BRMS1 transfection restores homotypic gap junctional intercellular communication in these human breast carcinoma cells. In turn, this implies that the cells are affected for their ability to detach from the primary tumor and/or respond to signals in transit or at the secondary site.

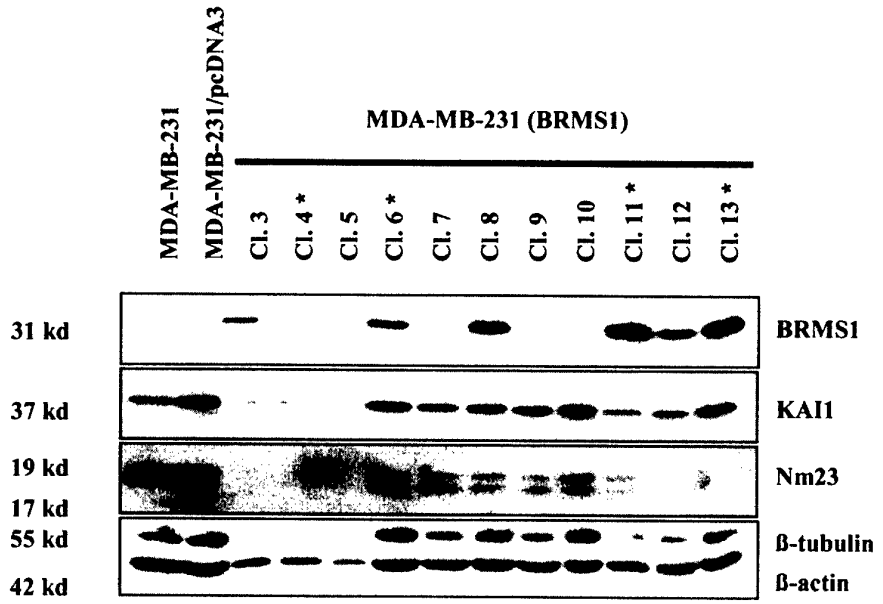

Figure 6. Immunoblot of MDA-MB-231 and MDA-MB 435 cell clones for determining BRMS1 expression. Protein (50 μg total protein/lane) was loaded. BRMS1 was detected using antibody to the SV40-901 epitope. To determine whether BRMS1 protein expression correlated with expression of known metastasis suppressor genes, the blot was stripped and re probed with antibodies/anti sera to human metastasis suppressor genes Kai1 and NM23, with β-tubulin and β-actin used to monitor equal loading. E-cadherin was not detectable in the parental or transfectant cell lines (data not shown). Likewise, KiSS1 expression did not correlate with BRMS1 expression in corresponding northern blots. *Indicates clones chosen for other studies.

BRMS1 is one of a growing number of genes whose expression appears to regulate metastasis specifically. Despite regulating this important cancer phenotype, the physiologic roles of these 'metastasis suppressors' are not yet known. Interestingly, many of the metastasis suppressors identified to date have mechanisms controlling cellular interactions [16], including BRMS1. The interplay between these proteins (and the pathways they represent) and those controlling adhesion, invasion, motility and proliferation will be fruitful areas of research.

Acknowledgements

This research was supported by grants CA 87728 and CA62168 from the National Institutes of Health to DRW. Support was also provided by the US Army Medical Research and Materiel Command DAMD-96-1-6152 (to DRW) and BC995879 (to HJD), the National Foundation for Cancer Research and the Jake Gittlen Memorial Golf Tournament. Dr R. Samant is supported by a postdoctoral fellowship from the US Army Medical Research and Materiel Command DAMD17-01-1-0362. Dr L. Shevde is supported by a postdoctoral fellowship from the Susan G. Komen Breast Cancer Research Foundation (PDF#2000-218). We are indebted to Drs Janet Price (MD Anderson Cancer Center) for providing the MDA-MB-435 and MDA-MB-231 cells; Satvir Tevethia (Penn State College of Medicine) for the anti-901 antibody; Fred Miller (Karmanos Cancer Center) for the MCF10A and MCF7 cells; Lisa Wei (Genvec Corporation) for the T47D^{co} cells; Stephen Ethier (U. Michigan Cancer Center) for the SUM cell lines; and Robert Clarke and Sandra McLeskey (Lombardi Cancer Center) for the LCC15 and MKL-4 cells.

References

1. Welch DR, Rinker-Schaeffer CW. What defines a useful marker of metastasis in human cancer? J Natl Cancer Inst 1999; 91 (16): 1351–3.
2. Welch DR, Wei LL. Genetic and epigenetic regulation of human breast cancer progression and metastasis. Endocrine-related Cancer 1998; 5 (3): 155–97.
3. Freije JM, MacDonald NJ, Steeg PS. Nm23 and tumour metastasis: basic and translational advances. Biochem Soc Symp 1998; 63: 261–71.
4. Lee J-H, Miele ME, Hicks DJ et al. *KiSS-1*, a novel human malignant melanoma metastasis-suppressor gene. J Natl Cancer Inst 1996; 88 (23): 1731–7.
5. Lee J-H, Welch DR. Suppression of metastasis in human breast carcinoma MDA-MB-435 cells after transfection with the metastasis suppressor gene, KiSS-1. Cancer Res 1997; 57: 2384–7.
6. Lee J-H, Miele ME, Hicks DJ et al. *KiSS-1*, a novel human malignant melanoma metastasis-suppressor gene. J Natl Cancer Inst 1997; 89 (20): 1549 [Erratum].
7. Phillips KK, White AE, Hicks DJ et al. Correlation between reduction of metastasis in the MDA-MB-435 model system and increased expression of the Kai-1 protein. Mol Carcinog 1998; 21 (3): 111–20.
8. Shindoh M, Higashino F, Kaya M et al. Correlated expression of matrix metalloproteinases and *ets* family transcription factor E1A-F in invasive oral squamous-cell- carcinoma-derived cell lines. Am J Pathol 1996; 148 (3): 693–700.
9. Mbalaviele G, Dunstan CR, Sasaki A et al. E-cadherin expression in human breast cancer cells suppresses the development of osteolytic bone metastases in an experimental metastasis model. Cancer Res 1996; 56 (17): 4063–70.
10. Yoshida BA, Dubauskas Z, Chekmareva MA et al. Identification and characterization of candidate prostate cancer metastasis-suppressor genes encoded on human chromosome 17. Cancer Res 1999; 59 (21): 5483–7.

11. Zou Z, Anisowicz A, Hendrix MJC et al. Maspin, a serpin with tumor-suppressing activity in human mammary epithelial cells. Science (Washington DC) 1994; 263 (5146): 526–9.
12. Zhang M, Shi Y, Magit D et al. Reduced mammary tumor progression in WAP-TAg/WAP-maspin bitransgenic mice. Oncogene 2000; 19 (52): 6053–8.
13. DeClerck YA, Perez N, Shimada H et al. Inhibition of invasion and metastasis in cells transfected with an inhibitor of metalloproteinases. Cancer Res 1992; 52 701–8.
14. Khokha R. Suppression of the tumorigenic and metastatic abilities of murine B16-F10 melanoma cells *in vivo* by the overexpression of the tissue inhibitor of metalloproteinases-1. J Natl Cancer Inst 1994; 86 (4): 299–304.
15. Seraj MJ, Samant RS, Verderame MF et al. Functional evidence for a novel human breast carcinoma metastasis suppressor, *BRMS1*, encoded at chromosome 11q13. Cancer Res 2000; 60 (11): 2764–9.
16. Yoshida BA, Sokoloff M, Welch DR et al. Metastasis-suppressor genes: a review and perspective on an emerging field. J Natl Cancer Inst 2000; 92 (21): 1717–30.
17. Price JE, Polyzos A, Zhang RD et al. Tumorigenicity and metastasis of human breast carcinoma cell lines in nude mice. Cancer Res 1990; 50 (3): 717–21.
18. Welch DR, Tomasovic SP. Implications of tumor progression on clinical oncology. Clin Exptl Metastasis 1985; 3: 151–88.
19. Fu TM, Bonneau RH, Epler M et al. Induction and persistence of a cytotoxic T lymphocyte (CTL) response against a herpes simplex virus-specific CTL epitope expressed in a cellular protein. Virology 1996; 222 (1): 269–74.
20. Kierstead TD, Tevethia MJ. Association of p53 binding and immortalization of primary C57BL/6 mouse embryo fibroblasts by using simian virus 40 T-antigen mutants bearing internal overlapping deletion mutations. J Virol 1993; 67 (4): 1817–29.
21. Welch DR. Technical considerations for studying cancer metastasis *in vivo*. Clin Exp Metastasis 1997; 15 (3): 272–306.
22. Rao VH, Singh RK, Bridge JA et al. Regulation of MMP-9 (92 kDa type IV collagenase/gelatinase B) expression in stromal cells of human giant cell tumor of bone. Clin Exp Metastasis 1997; 15 (4): 400–9.
23. Martelli AM, Tabellini G, Bortul R et al. Enhanced nuclear diacylglycerol kinase activity in response to a mitogenic stimulation of quiescent Swiss 3T3 cells with insulin-like growth factor I. Cancer Res 2000; 60 (4): 815–21.
24. Flanagan L, Van Weelden K, Ammerman C et al. SUM-159PT cells: a novel estrogen independent human breast cancer model system. Breast Cancer Res Treat 1999; 58 (3): 193–204.
25. Shafie SM, Formation of metastasis by human breast carcinoma cells (MCF7) in nude mice. Cancer Lett 1980; 11: 81–7.
26. Soule HD, Maloney TM, Wolman SR et al. Isolation and characterization of a spontaneously immortalized human breast epithelial cell line, MCF-10. Cancer Res 1990; 50 (18): 6075–86.
27. Pauley RJ, Soule HD, Tait L et al. The MCF10 family of spontaneously immortalized human breast epithelial cell lines: models of neoplastic progression. Eur J Cancer Prev 1993; 2 (Suppl 3): 67–76.
28. Thompson EW, Sung V, Lavigne M et al. LCC15- MB: a vimentin-positive human breast cancer cell line from a femoral bone metastasis. Clin Exp Metastasis 1999; 17 (3): 193–204.
29. Wei LL, Yang X, Phillips KK et al. Analysis of KAI-1 mRNA expression in human breast cancer cell lines. Proc Am Assoc Cancer Res 1996; 37 529.
30. Kurebayashi J, McLeskey SW, Johnson MD et al. Quantitative demonstration of spontaneous metastais by MCF7 human breast cancer cells cotransfected with fibroblast growth factor 4 and LacZ. Cancer Res 1993; 53 (9): 2178–87.
31. Stracke ML, Krutzsch HC, Unsworth EJ et al. Identification, purification, and partial sequence analysis of autotaxin, a novel motility-stimulating protein. J Biol Chem 1992; 267 (4): 2524–9.
32. Walther SE, Denhardt DT. Directed mutagenesis reveals that two histidines in tissue inhibitor of metalloproteinase-1 are each essential for the suppression of cell migration, invasion, and tumorigenicity. Cell Growth Differ 1996; 7 (11): 1579–88.
33. Lester BR, McCarthy JB. Tumor cell adhesion to the extracellular matrix and signal transduction mechanisms implicated in tumor cell motility, invasion and metastasis. Cancer Metastasis Rev 1992; 11 (1): 31–44.
34. Hernández-Alcoceba R, Del Peso L, Lacal JC. The Ras family of GTPases in cancer cell invasion. Cell Mol Life Sci 2000; 57 (1): 65–76.
35. Curran S, Murray GI. Matrix metalloproteinases: molecular aspects of their roles in tumour invasion and metastasis. Eur J Cancer [A] 2000; 36 (13): 1621–30.
36. Koblinski JE, Ahram M, Sloane BF. Unraveling the role of proteases in cancer. Clin Chim Acta 2000; 291 (2): 113–35.
37. Li L, Price JE, Fan D et al. Correlation of growth capacity of human tumor cells in hard agarose with their *in vivo* proliferative capacity at specific metastatic sites. J Natl Cancer Inst 1989; 81 (18): 1406–12.
38. Nicolson GL, Lembo TM, Welch DR. Growth of rat mammary adenocarcinoma cells in semisolid clonogenic medium not correlated with spontaneous metastatic behavior: Heterogeneity in the metastatic, antigenic, enzymatic and drug sensitivity properties of cells from different sized colonies. Cancer Res 1988; 48 (2): 399–404.
39. Leone A, Flatow U, King CR et al. Reduced tumor incidence, metastatic potential, and cytokine responsiveness of nm23-transfected melanoma cells. Cell 1991; 65 (1): 25–35.
40. Leone A, Flatow U, VanHoutte K et al. Transfection of human nm23-H1 into the human MDA-MB-435 breast carcinoma cell line: effects on tumor metastatic potential, colonization and enzymatic activity. Oncogene 1993; 8 (9): 2325–33.
41. Loewenstein WR, Kanno Y. Intercellular communication and the control of tissue growth: Lack of communication between cancer cells. Nature (London) 1966; 209 (29): 1248–9.
42. Yamasaki H, Mesnil M, Omori Y et al. Intercellular communication and carcinogenesis. Mutation Res Fundam Mol Mech Mutagenesis 1995; 333 (1–2): 181–8.
43. Ito A, Katoh F, Kataoka TR et al. A role for heterologous gap junctions between melanoma and endothelial cells in metastasis. J Clin Invest 2000; 105 (9): 1189–97.
44. El-Sabban ME, Pauli BU. Cytoplasmic dye transfer between metastatic tumor cells and vascular endothelium. J Cell Biol 1991; 115 (5): 1375–82.
45. Nicolson GL, Dulski KM, Trosko JE. Loss of intercellular junction communication correlates with metastatic potential in mammary adenocarcinoma cells. Proc Natl Acad Sci USA 1988; 85 (2): 473–6.
46. Donahue HJ. Gap junctions and biophysical regulation of bone cell differentiation. Bone 2000; 26 (5): 417–22.
47. Saunders MM, Seraj MJ, Li ZY et al. Breast cancer metastatic potential correlates with a breakdown in homospecific and heterospecific gap junctional intercellular communication. Cancer Res 2001; 61 (5): 1765–7.
48. Fidler IJ, Radinsky R. Genetic control of cancer metastasis. J Natl Cancer Inst 1990; 82: 166–8.
49. Fidler IJ, Radinsky R. Search for genes that suppress cancer metastasis. J Natl Cancer Inst 1996; 88 (23): 1700–3.

Experimental Cell Research **273,** 229–239 (2002)
doi:10.1006/excr.2001.5452, available online at http://www.idealibrary.com on IDEAL®

Donahue
Appendix 3

Suppression of Human Melanoma Metastasis by the Metastasis Suppressor Gene, *BRMS1*

Lalita A. Shevde,* Rajeev S. Samant,* Steven F. Goldberg,* Tabo Sikaneta,† Alessandro Alessandrini,† Henry J. Donahue,‡ David T. Mauger,§ and Danny R. Welch*,[1]

*Jake Gittlen Cancer Research Institute, ‡Department of Orthopaedics and Rehabilitation, and §Department of Health Evaluation Sciences, The Pennsylvania State University College of Medicine, Hershey, Pennsylvania 17033; and †Department of Molecular and Cellular Biology, Harvard University, Cambridge, Massachusetts 02138

We recently identified a novel metastasis suppressor gene, *BRMS1,* in breast cancer. Since the *BRMS1* gene maps to chromosome 11q13.1-q13.2 and since chromosome 11q defects have been described in various stages of human melanoma progression, we hypothesized that *BRMS1* may function as a tumor or metastasis suppressor in melanomas as well. Quantitative real-time RT-PCR revealed that *BRMS1* mRNA expression was high in melanocytes, considerably reduced in early melanoma-derived cell lines, and barely detectable in advanced/metastatic cell lines. Stable transfectants of *BRMS1* in the human melanoma cell lines MelJuSo and C8161.9 did not alter the tumorigenicity of either cell line, but significantly suppressed metastasis compared to vector-only transfectants. Orthotopic tumors continued to express *BRMS1,* but expression was lost in lung metastases. *In vitro* morphology, growth rate, and histology of BRMS1 transfectants were similar to controls. *BRMS1* transfectants were less invasive in a collagen sandwich assay and had restored homotypic gap junctional intercellular communication (GJIC). Thus, *BRMS1* functions as a metastasis suppressor in more than one tumor type (i.e., breast carcinoma and cutaneous melanoma) by modifying several metastasis-associated phenotypes. © 2002 Elsevier Science (USA)

Key Words: **melanoma; chromosome 11; *BRMS1;* metastasis; suppression; gap junctions; invasion.**

INTRODUCTION

Worldwide incidence of melanoma is increasing rapidly. More than 40,000 new cases of melanoma are reported annually and this tumor type accounts for nearly 5% of all cancer-related mortalities. If melanoma is diagnosed before it metastasizes, the 5-year survival rate is greater than 80%. Once metastasis has occurred, 5-year survival rate drops to <5% [1]. The transition from a nonmalignant to a malignant form of melanoma is characterized by genetic instability and the appearance of numerous chromosomal abnormalities [reviewed in 2]. The identities of specific genes responsible for the conversion of benign to malignant are only recently beginning to be identified.

Control of the multistep metastatic cascade involves an interplay between many genes. Metastasis-regulatory genes can be classified as metastasis-promoting (i.e., genes that drive the conversion of a non-metastatic tumor to metastatic) and metastasis-suppressing. Metastasis suppressor genes, although akin to tumor suppressors, are distinct in that they block the spread of the tumor cells without affecting primary tumor formation. A tumor suppressor, on the other hand, also blocks metastasis since tumorigenicity is a prerequisite to metastasis [3, 4]. Interestingly, while metastasis requires coordinated expression of many genes, it takes only one gene to inhibit metastasis at any step of the cascade [3, 4].

Of particular relevance for this study, genetic alterations involving the long arm of chromosome 11 are implicated in melanoma pathogenesis and progression [2]. Robertson *et al.* provided early functional evidence for a melanoma tumor suppressor on human chromosome 11 [5]. Briefly, introduction of an intact copy of chromosome 11 by microcell transfer severely retarded the ability of the metastatic human melanoma cell line MelJuSo to grow in culture and moderately reduced growth of UACC903 cells *in vitro.* The ability of hybrid cells to form subcutaneous tumors in athymic mice was significantly suppressed. They further mapped a melanoma tumor suppressor to the long arm of chromosome 11, but the identity of the tumor suppressor remains unknown.

We recently cloned a human breast cancer metastasis suppressor gene, *BRMS1* (Accession No. AF159141), using differential display to compare metastasis-competent MDA-MB-435 cells with metastasis

[1] To whom correspondence and reprint requests should be addressed at Jake Gittlen Cancer Research Institute, Mailstop H059, The Pennsylvania State University College of Medicine, 500 University Drive, Hershey, PA 17033-2390. E-mail: drw9@psu.edu.

0014-4827/02 $35.00
© 2002 Elsevier Science (USA)
All rights reserved.

suppressed chromosome 11-MDA-MB-435 hybrids [6]. Transfection of full-length *BRMS1* cDNA into MDA-MB-435 or MDA-MB-231 cells significantly suppressed metastasis without affecting tumorigenicity [6]. Likewise, transfection and constitutive expression of the murine ortholog suppressed metastasis of murine mammary carcinomas [7]. The *BRMS1* gene mapped to human chromosome 11q13. While slightly proximal (centromeric) to one of the regions Robertson *et al.* reported for a melanoma tumor suppressor, *BRMS1* was sufficiently close to justify examining whether it might exert a novel function in melanoma (i.e., tumor suppression) or whether it would function as a metastasis suppressor.

MATERIALS AND METHODS

Cell Lines

MelJuSo (a gift from Dr. J. Johnson, Institute of Immunology, University of Munich) is an amelanotic human melanoma cell line capable of forming metastases in regional lymph nodes and lungs after subcutaneous or intradermal injection into 3- to 5-week-old female athymic mice [8, 9].

Parental C8161 is an aggressive, metastatic, amelanotic human melanoma cell line derived from an abdominal wall metastasis [10]. C8161.9 is a highly metastatic clone obtained by limiting dilution cloning of C8161 [11].

MelJuSo and C8161.9 were cultured in a 1:1 mixture of Dulbecco's-modified minimum essential medium and Ham's F-12 medium (DME-F12; Invitrogen, Gaithersburg, MD), supplemented with 5% fetal bovine serum (FBS; Atlanta Biologicals, Atlanta, GA), 1% non-essential amino acids (Invitrogen, San Diego CA), 1.0 mM sodium pyruvate, but no antibiotics or antimycotics.

Full-length *BRMS1* cDNA (see below) cloned into the constitutive mammalian expression vector, pcDNA3 (Invitrogen), was transfected into MelJuSo and C8161.9. Transfected cells were selected and maintained in DME-F12 + 5% FBS containing 500 μg/ml geneticin (G-418; Invitrogen). Cell cultures were maintained at 37°C in a humidified atmosphere with 5% CO_2. Cultures were passaged using a solution of 2 mM EDTA in Ca^{+2}/Mg^{+2}-free Dulbecco's phosphate-buffered saline (CMF-DPBS; Invitrogen) when they reached 80–90% confluence. Transfectant clones were used between passages 7 and 11 in order to minimize the impacts of clonal diversification and phenotypic instability [12, 13]. For all functional and biological assays, cells with viability >95% were used at 70–90% confluence. All the lines were routinely checked and found negative for *Mycoplasma spp.* contamination using TaKaRa Mycoplasma detection kit (Panvera, Madison, WI).

Transfection

BRMS1 ± SV40T epitope 901 [14, 15] fused in-frame to the N-terminus was cloned into constitutive mammalian expression vector pcDNA3 (Invitrogen) under control of the cytomegalovirus promoter. Briefly, cells were detached using a 2 mM EDTA solution, plasmid DNA (10 μg) was added to the cells, and the mixture was placed onto ice for 5 min before electroporation. Following electroporation (Bio-Rad, Hercules, CA; 220 V, 960 μFd, $\infty\Omega$), cells were chilled on ice for 10 min prior to plating. One day later, transfectants were selected by addition of culture medium containing G-418 (500 μg/ml). Single-cell clones were isolated by limiting dilution in 96-well plates. Stable transfectants were assessed for expression of transcripts by Northern blotting and/or immunoblotting. Individual clones were used for *BRMS1* transfectants and some vector-only transfectants. Mixtures of vector-only transfectant clones were used for some experiments.

Immunoblotting

BRMS1 protein expression was determined by collecting total protein of 70–90% confluent cell cultures. Following aspiration of medium, plates were rinsed three times with CMF-DPBS before addition of 1 ml lysis buffer (50 mM Tris–HCl, 0.1% Triton X-100, pH 6.8). Lysates were cleared by centrifugation at 10,000*g* at 4°C for 15 min. Protein concentration was determined using the Bradford method [16]. Protein (20–30 μg/lane) was mixed with 5× loading buffer (50% glycerol, 1.5% bromphenol blue, 2% β-mercaptoethanol, 2% SDS) and separated by 12% SDS–PAGE. Protein was transferred to Poly Screen membrane (NEN-Dupont, Boston, MA) by semidry transfer (5.5 mA/cm^2, 20 V, 30 min). Following fixation of proteins (air drying for 15 min at room temperature), the membrane was wetted in methanol, rinsed in distilled water, and blocked in a TTBS solution (0.05% Tween 20, 20 mM Tris, 140 mM NaCl, pH 7.6) containing 5% dry nonfat milk for 1 h. The 901-tagged BRMS1 was detected using a monoclonal anti-901 antibody (generously provided by Dr. S. Tevethia, Department of Microbiology and Immunology, Pennsylvania State University College of Medicine) at a final dilution of 1:5000 for 1 h with constant agitation. Membranes were then washed with TTBS and probed with 1:10,000 dilution of sheep anti-mouse secondary antibody conjugated to horseradish peroxidase (Amersham-Pharmacia Biotech, Piscataway, NJ) in a solution of 5% nonfat dry milk/TTBS for 1 h at room temperature before washing in TTBS. Bound secondary antibodies were detected using chemiluminescence (ECL Amersham-Pharmacia Biotech) for 30 s to 10 min. Some of the blots were reprobed with anti-β-actin antibody (Sigma-Aldrich, St. Louis, MO) after being stripped using a solution of 200 mM glycine, 50 mM potassium acetate, and 0.2% β-mercaptoethanol, pH 4.5, to evaluate equal loading.

In Vitro Growth Characterization

Cells at 80–90% confluence were detached using 2 mM EDTA and seeded at a density of 2×10^4 cells/ml. The growth of cells was monitored daily for 10 days. Cell number was determined at each time point with the aid of a hemocytometer. Cell viability was also determined by cell morphology. Each day the morphology was recorded using an inverted microscope (Nikon Diaphot) equipped with a digital camera (Leica Microsystems Ltd. DC Viewer Version 3.2.0.0 (Heerbrugg, Germany).

Metastasis Assays

Two assays were employed to measure metastasis. "Experimental" metastasis involved intravenous inoculation of cells, whereas for "spontaneous" metastasis, cells were injected intradermally or subcutaneously.

Experimental metastasis assay. Immediately prior to injection, cells at 80–90% confluence were detached with 2 mM EDTA solution, washed with chilled CMF-DPBS, counted using a hemocytometer and resuspended in ice-cold Hanks' balanced salt solution (HBSS; Invitrogen) to a final concentration of 1.0×10^6 cells/ml. Melanoma cells and vector-only and BRMS1 transfectants (0.2×10^6 in 0.2 ml) were injected into the lateral tail vein of 3- to 4-week-old, female athymic mice (Harlan Sprague-Dawley, Indianapolis, IN) using a 27-gauge needle affixed to a 1-cc tuberculin syringe. Mice were killed 4–5 weeks postinjection and examined for the presence of metastases. Lungs were removed, rinsed in water, and fixed in diluted Bouin's solution (20% Bouin's fixative in neutral buffered formalin) before quantification of surface metastases [12]. A small portion of the lungs was also stored in RNAlater (Ambion, Austin, TX) for analysis of BRMS1 expression.

Spontaneous metastasis assay. Similarly detached cells (1×10^6) were injected intradermally into the dorsolateral flanks of athymic mice. Tumor size was measured weekly and mean tumor diameter calculated by taking the square root of the product of orthogonal measurements. After the mean tumor diameter reached 1.0–1.5 cm, tumors were surgically removed under ketamine:xylazine (80–85: 14–16 mg/kg) anesthesia and the wounds were closed with sterile stainless-steel clips (9 mm; Becton-Dickinson, Sparks, MD). Four weeks later, mice were killed. Tumor tissue and lung metastases were preserved in neutral buffered formalin or diluted Bouin's fixative histologic analysis. Sections (4–6 μm) were prepared by dehydration, paraffin embedding, sectioning, and staining with hematoxylin and eosin. Grossly visible surface lung metastases were counted as above. Tissue from the locally growing tumor was also stored in RNAlater.

Animals were maintained under the guidelines of the National Institute of Health and the Pennsylvania State University College of Medicine. All protocols were approved and evaluated by Institutional Animal Care and Use Committee. Food and water were provided *ad libitum.* All experiments were repeated at least twice using a minimum of eight mice per group. The number of lung metastases were compared using one-way analysis of variance followed by the Student Newman–Keuls posttest to determine significance. P values less than 0.05 were considered statistically significant.

Scrape Loading Dye Transfer Assay

For an assessment of homotypic GJIC, cell lines were scrape loaded and assessed for dye transfer [17]. Briefly, cells were grown to 75–85% confluence in six-well culture plates (Corning, Oneata, NY). Cells were rinsed three times with a phosphate-buffered saline solution containing Ca^{2+} and Mg^{2+} before scrape loading. The cell monolayer was loaded with two fluorescent dyes (0.5% Lucifer yellow (LY (Sigma-Aldrich); M_r 457 Da), which can penetrate gap junction channels, and 0.5% rhodamine dextran (RD (Sigma-Aldrich); M_r 10 kDa), which is too large to pass through the channels) by scratching with a 26-gauge needle. RD thus identifies the cells originally receiving the dyes. Following incubation for 10 min at 37°C, cells were washed with PBS before adding 2 ml medium. Cells were examined using a fluorescent microscope (Leica DC Viewer Version 3.2.0.0; Leica Microsystems Ltd., Heerbrugg, Germany) fitted with $\lambda_{excitation}$ = 480 ± 20 and 535 ± 25 nm and $\lambda_{emission}$ = 535 ± 25 and 610 ± 37.5 nm filters.

Collagen Sandwich Assay

An 80% solution of rat tail type I collagen (Becton-Dickinson, San Diego, CA) in DME-F12, pH 7.5, was used to coat six-well tissue culture plates. Excess solution was drained. Plates were allowed to set at 37°C for 15 min. Cells (5×10^4/ml) were suspended in 3 ml of 80% collagen solution in DME-F12 containing 10% FBS before placement into the tissue culture plates. After incubation for 1 h at 37°C, another coat of collagen was poured onto the plate. After setting for 15 min at 37°C, excess collagen solution was drained, and plates were returned to a humidified CO_2 incubator. Cells were examined daily for 5 days to note any morphological changes.

RNA Isolation and Reverse Transcriptase (RT)-PCR

Following flash-freezing in liquid nitrogen, RNA was extracted from the lungs of athymic mice showing metastases and primary tumor tissue using TRIzol (Invitrogen) according to manufacturer's instructions. An RT-PCR was set up using total RNA (5 μg) with human *BRMS1*-specific primers HSPF01 (5′-ACTGAGTCAGCTGCGGTTGCGG) and HSPR02 (5′-AAGACCTGGAGCTGCCTCTGGCGTGC) and human G3PDH control amplimer set (Clontech, Palo Alto, CA). The products were resolved on a 1% agarose gel and visualized by ethidium bromide staining.

Northern Blot Hybridization

Total RNA (20 μg) was size separated on 1% agarose formaldehyde gels before transferring onto a positively charged Hybond-N^+ nylon membrane (Amersham Life Sciences, Arlington Heights, IL) using the Turboblotter system (Schleicher & Schuell, Keene, NH) and fixed by UV cross-linking. Random prime- (RediPrime, Amersham-Pharmacia) labeled *BRMS1* cDNA was used as a probe. All prehybridizations and hybridizations were carried out at 68°C using ExpressHyb solution (Clontech) according to manufacturer's recommendations. The membranes were exposed to Kodak BioMax MR X-ray film (Rochester, NY). Equal loading and transfer efficiency were assessed by hybridizing the blots with human G3PDH cDNA (*PstI*/*KpnI* 780-bp fragment ATCC57090/ATCC57091 (American Type Culture Collection, Manassas, VA) in pBR322).

Real-Time PCR

BRMS1 expression was determined in melanoma cell lines derived from different pathological stages (generously provided by Dr. M. Herlyn, Wistar Institute, Philadelphia, PA) by a real-time quantitative RT-PCR (RTQ) with a Perkin–Elmer ABI Prism 7700 sequence detection system (Shelton, CT). The forward and reverse primers used for *BRMS1* are 5′-TGCAGCGGAGCCTCAAG-3′ and 5′-TCACATCCAGACAGAAGCCCT-3′, respectively. For quantifying the mRNA with real-time PCR, the probe for *BRMS1* 5′-TTCGCATTCAGGTGGCAGGGATCTA-3′ was labeled with a reporter fluorescent dye 6-carboxyfluorescein (FAM) at its 5′ end and the 3′ end was labeled with Black Hole quencher (Biosearch Technologies, Inc., Novato, CA). The primers and probe were designed using the PE/ABD Primer Express software. Probes were synthesized by Biosearch Technologies, Inc.

Following extraction of RNA from cells using TRIzol (Invitrogen), RT reaction was performed using the TaqMan Universal Master Mix buffer and MuLV reverse transcriptase (Perkin–Elmer Applied Biosystems, Wellesley, MA). RT was carried out for 60 min at 42°C followed by incubation at 72°C for 5 min and 25°C for 2 min.

Real-time PCR was done using the TaqMan universal PCR assay mix in a 96-well reaction plate. G3PDH was amplified at the same time and used as a reference gene. Following reverse transcription, an aliquot was run with specific probes and primers. Each RT-PCR contained the following: 10 μM BRMS1-specific primers, 1 μM BRMS1-fluorogenic probe, 10 μM G3PDH-specific primers, 1 μM G3PDH probe, and 8 μl of the reverse transcriptase product. Following incubation for 2 min at 50°C and 10 min at 95°C, PCR amplification was performed for 40 cycles (95°C for 15 s and 60°C for 1 min). All reactions were carried out in triplicate using the ABI Prism 7700 SDS. The threshold cycle C_T values were measured and calculated by computer software (Perkin–Elmer ABI) and averaged from the values obtained from each reaction.

Real-time PCR quantification. The expression of *BRMS1* (C_{TS}) was normalized to an endogenous reference gene (G3PDH). C_{TS} was calculated by subtracting the C_T value of the reference (C_{TR}) from the C_T value of the sample (ΔC_T; $\Delta C_T = C_{TS} - C_{TR}$). The relative expression ($2^{-\Delta\Delta CT}$) to a calibrator (placenta RNA; Clontech) was determined by subtracting the $\Delta C_{T(Calibrator)}$ from the ΔC_T value ($\Delta\Delta C_T = \Delta C_T - \Delta C_{T(Calibrator)}$).

RESULTS AND DISCUSSION

Karyotypic and molecular data indicate that genetic alterations of chromosome 11q are involved in the pathogenesis of malignant melanoma as well as of other malignancies [18–21]. Loss of heterozygosity (LOH) studies have implicated one or more gene(s) in a broad area of 11q involved in the development of cuta-

TABLE 1

Expression of BRMS1 in Melanoma Cell Lines Analyzed by Real-Time PCR

	Average C_{Ts}	SD	Average C_{TR} (G3PDH)	SD (G3PDH)	ΔC_T	$\Delta\Delta C_T$	$2^{-\Delta\Delta CT}$	SD
Placental RNA (Clontech)	33.49	0.25	30.65	0.13	2.764	0	1.0	0.23
Melanocytes	35.34	0.11	36.85	0.31	−1.393	−4.157	17.998	2.84
WM793 (early VGP)	32.39	2.53	33.40	2.26	0.463	−2.301	4.987	0.89
WM115 (VGP)	33.74	0.22	30.99	0.22	2.857	−0.264	0.948	0.17
WM1205LU (metastatic)	32.85	0.18	29.23	0.17	3.817	1.053	0.483	0.03
WM239A (metastatic)	33.05	0.11	28.90	0.18	4.147	1.383	0.387	0.06

Note. Contains raw data from RTQ. The relative level of BRMS1 decreases with an increase in metastatic potential. A quantitative real-time PCR was done using placental RNA (Clontech, Palo Alto, CA) as a "calibrator" and GAPDH as an endogenous "reference."

neous melanoma [2]. *BRMS1* was sufficiently close to these loci to warrant evaluation of its role as either a tumor or metastasis suppressor gene in melanoma. Before embarking on functional studies, we first tested whether *BRMS1* expression was correlated with metastatic potential.

BRMS1 levels were measured in a panel of melanocyte- and melanoma-derived cell lines representing a continuum of melanoma stages of progression [22, 23] by quantitative real-time RT-PCR. Expression was normalized to placental RNA (Table 1, Fig. 1). Expression was highest in melanocytes and decreased as metastatic potential increased. This observation suggested a role for *BRMS1* in melanoma progression, rather than tumorigenesis. To test a role for *BRMS1* in melanoma cell behavior, *BRMS1* was transfected and overexpressed in metastatic cell lines having low levels of resident *BRMS1*. Initial studies utilized MelJuSo since chromosome 11 was previously shown to suppress growth and tumorigenicity [5]. Following transfection into MelJuSo, four clones were selected for follow-up experimentation because of different RNA expression that corresponded well with protein expression (Figs. 2A and 2B). *BRMS1* did not overtly alter *in vitro* morphology (Fig. 2C) but clone 20, the highest expressor, did lag in growth slightly (Fig. 2D). Similar findings were observed for transfectants of another metastatic human melanoma cell line C8161.9 (data not shown).

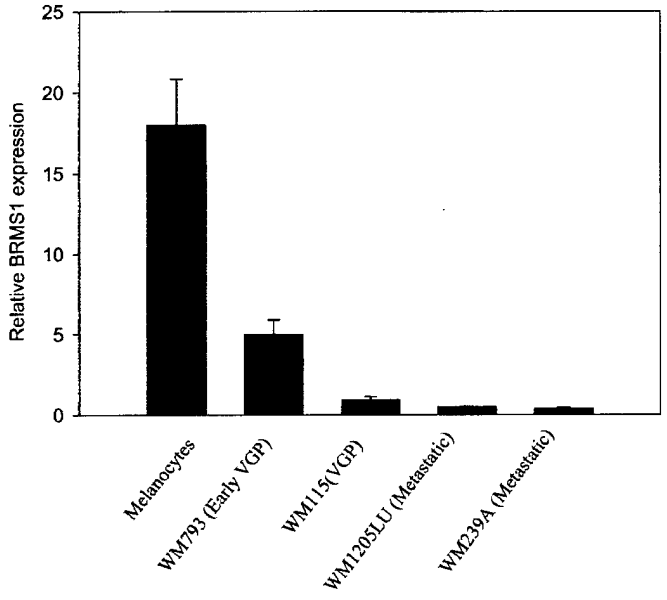

FIG. 1. BRMS1 levels decrease in cell lines representing stages of melanoma progression. Real-time RT-PCR was used to measure BRMS1 mRNA levels. Values are normalized to a human placenta control.

Parental MelJuSo, vector-only, and *BRMS1* transfectants formed tumors in every animal injected intradermally. Tumor growth rates were comparable between groups (Fig. 3A). Tumors were all densely nucleated and exhibited central necrosis regardless of the level of *BRMS1* expression. There was no noteworthy difference with regard to local invasion at the microscopic level (Fig. 3B). Initially, therefore, *BRMS1* did not appear to function as a tumor suppressor or as an inhibitor of local invasion.

A role for *BRMS1* in metastasis was difficult to assess because of low baseline incidence and the typically high variability associated with the spontaneous metastasis assay. Therefore, MelJuSo, vector-only transfectants, and *BRMS1*-transfected clones were examined for their abilities to form lung metastases following intravenous injection into the lateral tail vein of athymic mice (Fig. 3C). Reflective of inherent heterogeneity within the MelJuSo population, metastatic potential varied significantly for vector-only and *BRMS1* transfectants. Metastatic potentials for all *BRMS1* transfectant clones were at the lowest end of the spectrum with regard to metastatic lung colonization. That is, all were of equal or lesser metastatic capacity than the least metastatic control cell clone. Since it is extremely unlikely that all *BRMS1* transfectants were derived from only the least metastatic cells, these results suggested that *BRMS1* was a metastasis suppressor. Nonetheless, the variability among control clones made a definitive conclusion dif-

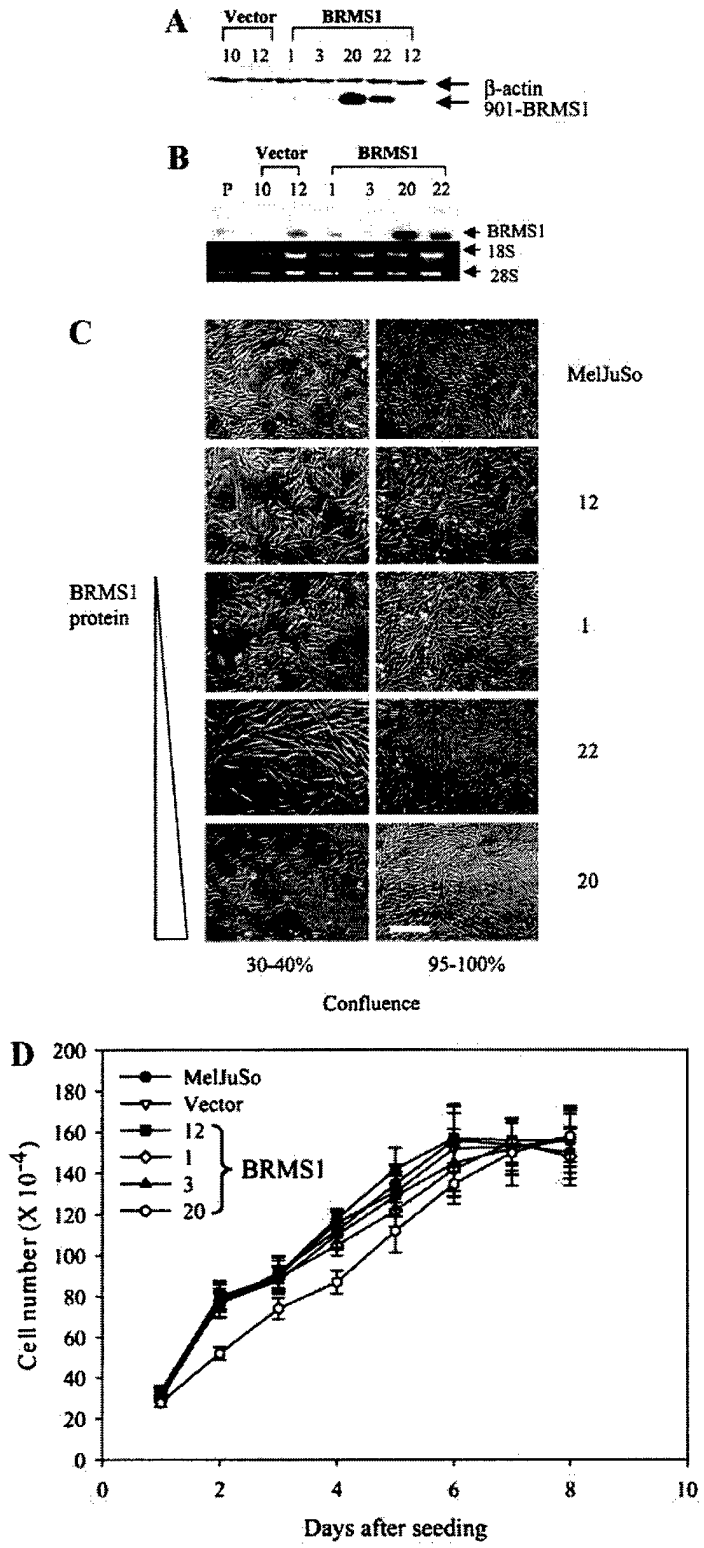

FIG. 2. Expression of BRMS1 by MelJuSo, vector-only control, and *BRMS1* transfectants by protein (A) and RNA (B) blots. Protein (~25 μg) was resolved on a 12% polyacrylamide gel. An immunoblot was probed with a monoclonal antibody to the SV40T 901 epitope. Equal loading was confirmed using β-actin (protein) or 18S and 28S RNA. Total RNA resolved on a 1% agarose formaldehyde gel and probed with radiolabeled full-length *BRMS1* cDNA. (B) A single specific band was seen at 1.5 kb corresponding to *BRMS1*. Lanes P, MelJuSo; vector, pcDNA3. (C) *In vitro* morphology of MelJuSo and *BRMS1* transfectants are similar. Relative BRMS1 expression is depicted by the triangle. (Bar, 200 μm; magnification 100×.) (D) *BRMS1* transfectants of MelJuSo display similar growth rates *in vitro*. Cells (2×10^4) were seeded in six-well culture plates and counted daily thereafter.

ficult until it was shown that *BMRS1* expression was lost or significantly decreased in the lung metastases (Fig. 3D). Only MelJuSo-BRMS1 clone 3 showed residual levels of *BRMS1* expression in the lung metastases evaluated using semiquantitative RT-PCR.

In order to partially compensate for clonal heterogeneity, we decided to study *BRMS1* in a more recently isolated, highly metastatic melanoma cell subclone. C8161.9 was recently isolated by limiting dilution from the human melanoma cell lines C8161 [11]. Even though clonal diversification does already exist [13], the extent of heterogeneity would theoretically be limited compared to a long-term culture. Following transfection with BRMS1, three clones of C8161.9 were selected based on their expression of BRMS1 protein (Fig. 4A). *BRMS1*-expressing C8161.9 transfectants were significantly suppressed for experimental metastases in athymic mice compared to the parental cell line or vector-only transfectants (Fig. 4B). There was also a trend towards expression-dependent inhibition in this cell line. As in MelJuSo, *BRMS1* transfectants were not significantly suppressed for intradermal tumor growth (Fig. 4C). The rates of growth for the *BRMS1* transfectants fell between those of metastatic C8161 cell clones [11]. Importantly, spontaneous metastases were less in *BRMS1* transfectants (Fig. 4D). *BRMS1* expression was retained in the primary tumor as determined by RT-PCR using human BRMS1-specific primers (Fig. 4E).

Collectively, the observations show that *BRMS1* suppresses experimental as well as spontaneous metastasis without blocking tumor growth. This meets the criteria of a melanoma metastasis suppressor [3, 4]. As with most other metastasis suppressors, the mechanisms by which they work are not well understood. We, therefore, performed a series of studies to define roles for *BRMS1* in suppressing melanoma metastasis.

Compared to parental or vector-only transfectants, *BRMS1* transfectants exhibit a lower invasive potential in a collagen sandwich assay. The collagen sandwich assay is an adaptation of the Matrigel invasion assay which has previously been used to measure invasion and has been correlated with metastasis [24, 25]. The collagen sandwich assay utilizes relatively inexpensive rat tail collagen rather than Matrigel and has been used to study the formation of invasive cellular extensions by renal cells (P. G. Linde, M. Andreucci,

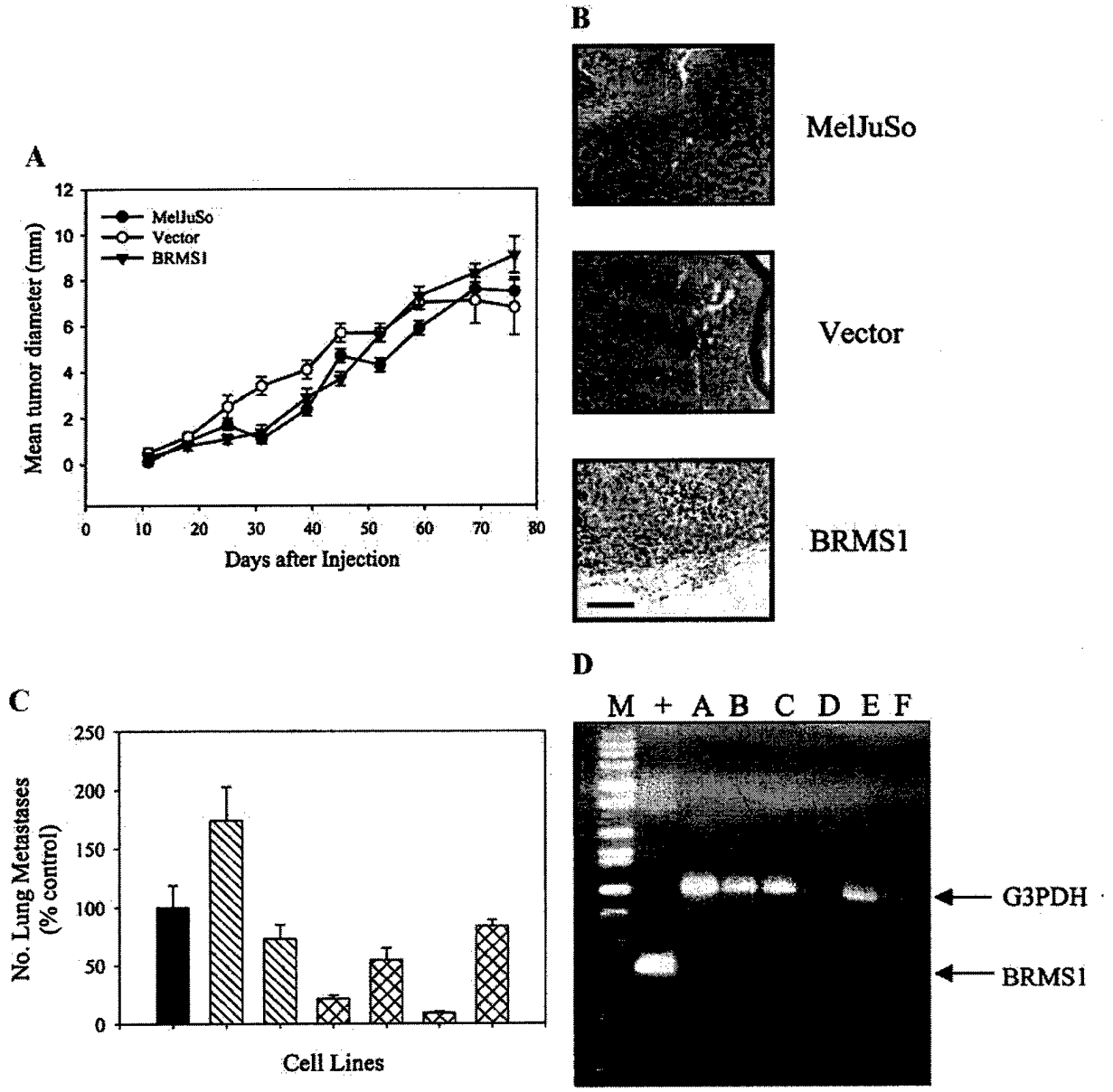

FIG. 3. (A) *BRMS1* transfectants of MelJuSo are not altered for tumor growth rate at orthotopic sites in athymic mice. Cells (1×10^6) were injected into the dorsolateral flank of 4- to 5-week-old female mice and mean tumor diameter was determined by taking the square root of the product of orthogonal measurements. (B) *BRMS1* does not significantly alter histologic features of MelJuSo. Note: parental, vector-only, and BRMS1 transfectant cells are locally invasive (bar, 200 μm). (C) *BRMS1* suppresses experimental lung metastasis of MelJuSo. Cells (2×10^5 cells/0.2 ml) were injected into the lateral tail vein. Bars (left to right), solid (MelJuSo parent); diagonal stripped (vector-only tranfectant clones 10 and mixed pool); cross-hatched (*BRMS1*-transfectant clones 1, 3, 20, and 22). Thirty days postinjection mice were killed and examined for the presence of metastasis. (D) *BRMS1* expression is lost in lung metastases. Total RNA from lung metastases were extracted and *BRMS1* mRNA expression was determined by RT-PCR using human-specific *BRMS1* primers. Human-specific G3PDH was used as a loading control. Lane M, molecular weight markers; lane +, positive control for BRMS1 (MelJuSo-BRMS1.20 RNA from cell culture); lane A, positive control for G3PDH; lane B, MelJuSo-vector control; lanes C–F, MelJuSo-BRMS1 clones 1, 3, 20 and 22, respectively. *BRMS1* transfectants are significantly different from control and vector-only transfectants ($P < 0.05$) by one-way ANOVA and Student Newman–Keuls posttest.

T. Sikaneta, R. Pioquinto, C. Cheung, T. Matsui, A. Rosenzweig, G. Choukroun, A. Arnaut, J. V. Bonventre, and A. Alessandrini, manuscript in preparation). The collagen sandwich assay was used to characterize the melanoma *BRMS1* transfectants for invasive properties. Cells were introduced into the assay in a blinded manner and morphology was monitored. As seen in Fig. 5, vector-only controls of both MelJuSo and C8161.9 form distinct cellular processes and extensions which are discernible even 24 h after seeding, but which become more evident after 5 days of incubation. *BRMS1* transfectants, on the other hand, form more

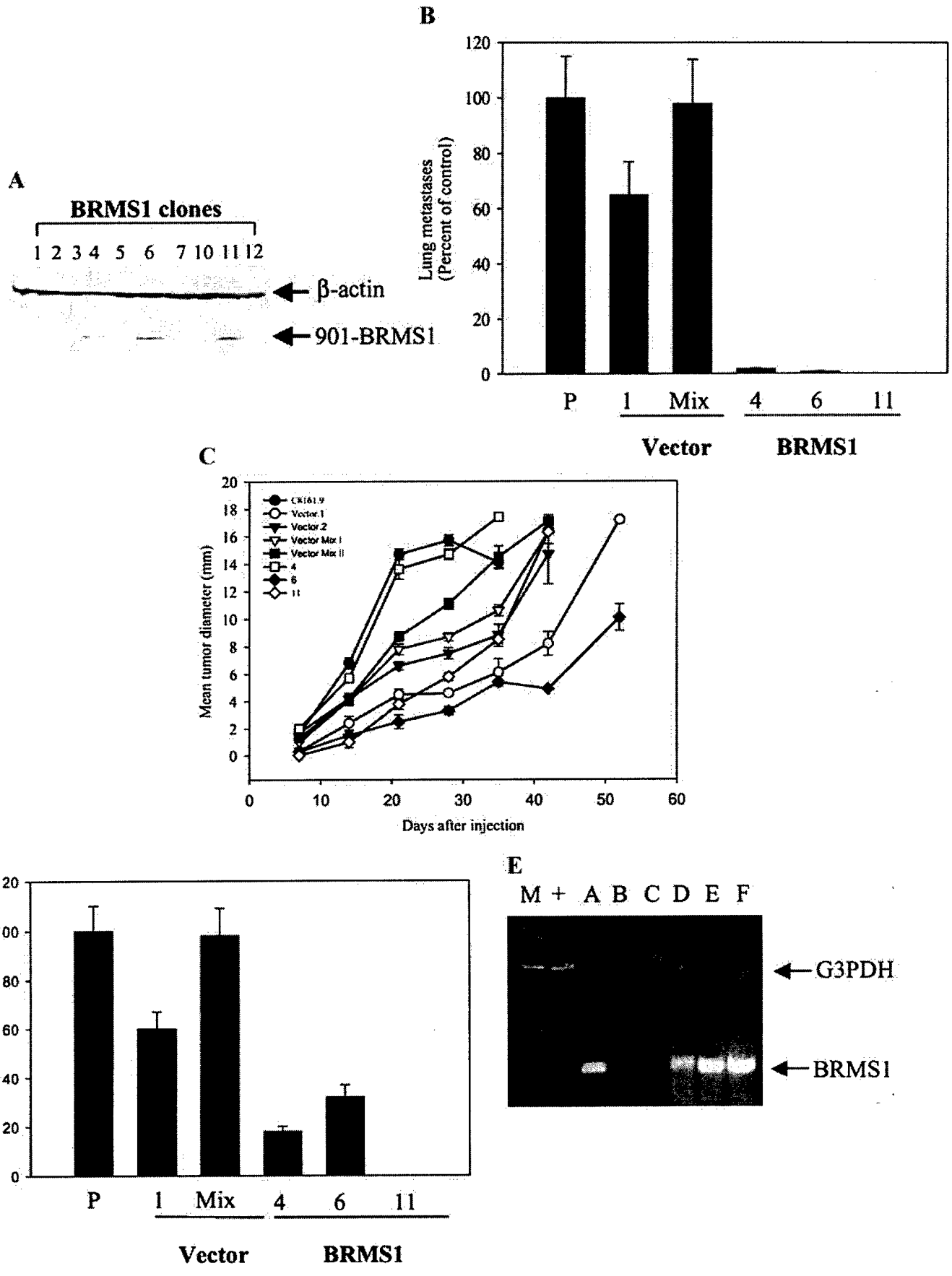
A
BRMS1 clones
1 2 3 4 5 6 7 10 11 12
β-actin
901-BRMS1
B
Lung metastases (Percent of control)
120
100
80
60
40
20
0
P 1 Mix 4 6 11
Vector
BRMS1
C
Mean tumor diameter (mm)
Days after injection
0 10 20 30 40 50 60
Vector.1
Vector.2
Vector Mix I
Vector Mix II
4
6
11
D
Lung metastases (Percent of control)
120
100
80
60
40
20
0
P 1 Mix 4 6 11
Vector
BRMS1
E
M + A B C D E F
G3PDH
BRMS1

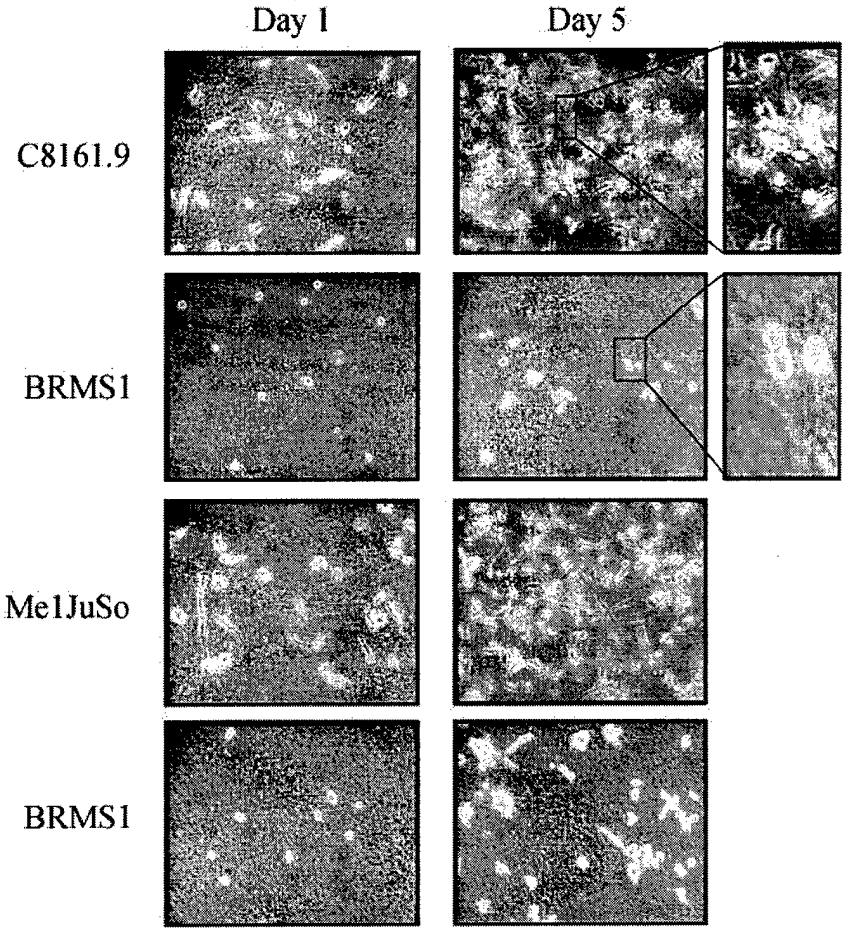

FIG. 5. *BRMS1* transfectants exhibit decreased tube formation and invasion in three-dimensional collagen cultures. Cells were sandwiched between layers of type I collagen and monitored daily for 5 days to observe morphological changes. Metastatic cells display formation of cellular processes, whereas *BRMS1* transfectants cluster and form spheroid-like masses.

spheroid-like masses without many cellular extensions. Images in Fig. 5 are representative of results with several clones seeded, but do not completely reflect the three-dimensional nature of the assay. Like the Matrigel assay, the collagen sandwich system offers a relatively simple, inexpensive surrogate for studying invasion and/or metastasis. The relationship is not perfect and does not yet have a biochemical and molecular explanation. The assay may prove useful in studying structure–activity relationships of *BRMS1.*

Interestingly, local invasion does not appear significantly different *in vivo.* Histologic evidence of tumor cell migration away from the primary tumor is evident in *BRMS1*-transfected breast carcinomas [6] and melanomas (data not shown). The reasons for this discrepancy are not yet understood and may reflect redundancy in the processes involved.

We previously showed that *BRMS1* restores GJIC in metastatic breast carcinoma cell lines [26]. To see whether GJIC was similarly altered in *BRMS1* transfectants, GJIC was evaluated in the melanoma transfectants by the scrape loading-dye transfer assay. The

FIG. 4. (A) Expression of *BRMS1* protein in C8161.9, vector-only control, and *BRMS1* transfectants. BRMS1 was detected using the SV40T-901 epitope. β-Actin was used as a loading control for the immunoblot. *BRMS1* suppresses experimental (B) and spontaneous (D) metastasis of C8161.9 without suppressing orthotopic tumor growth (C). Parental, vector-only (clone 1 (and clone 2 in C) and a mixture (MIX) of transfected clones), and *BRMS1*-transfectants clones (4, 6, and 11) were used for all experiments. Experimental lung colonization was determined following injection of 2×10^5 cells into the lateral tail vein. Spontaneous metastases and tumor growth were assessed following injection of 1×10^6 cells into an orthotopic dorsolateral site. To ensure that *BRMS1* is not a tumor suppressor, mRNA levels were assessed in locally growing tumors (E). Lane M, molecular weight markers; lane +, positive control for human-specific G3PDH; lane A, positive control for *BRMS1;* lanes B and C, C8161.9 vector (pcDNA3) controls; lanes D–F, C8161.9-BRMS1 clones 4, 6, and 11, respectively. *BRMS1* transfectants are significantly different from control and vector-only transfectants ($P < 0.05$) by one-way ANOVA and Student Newman–Keuls posttest.

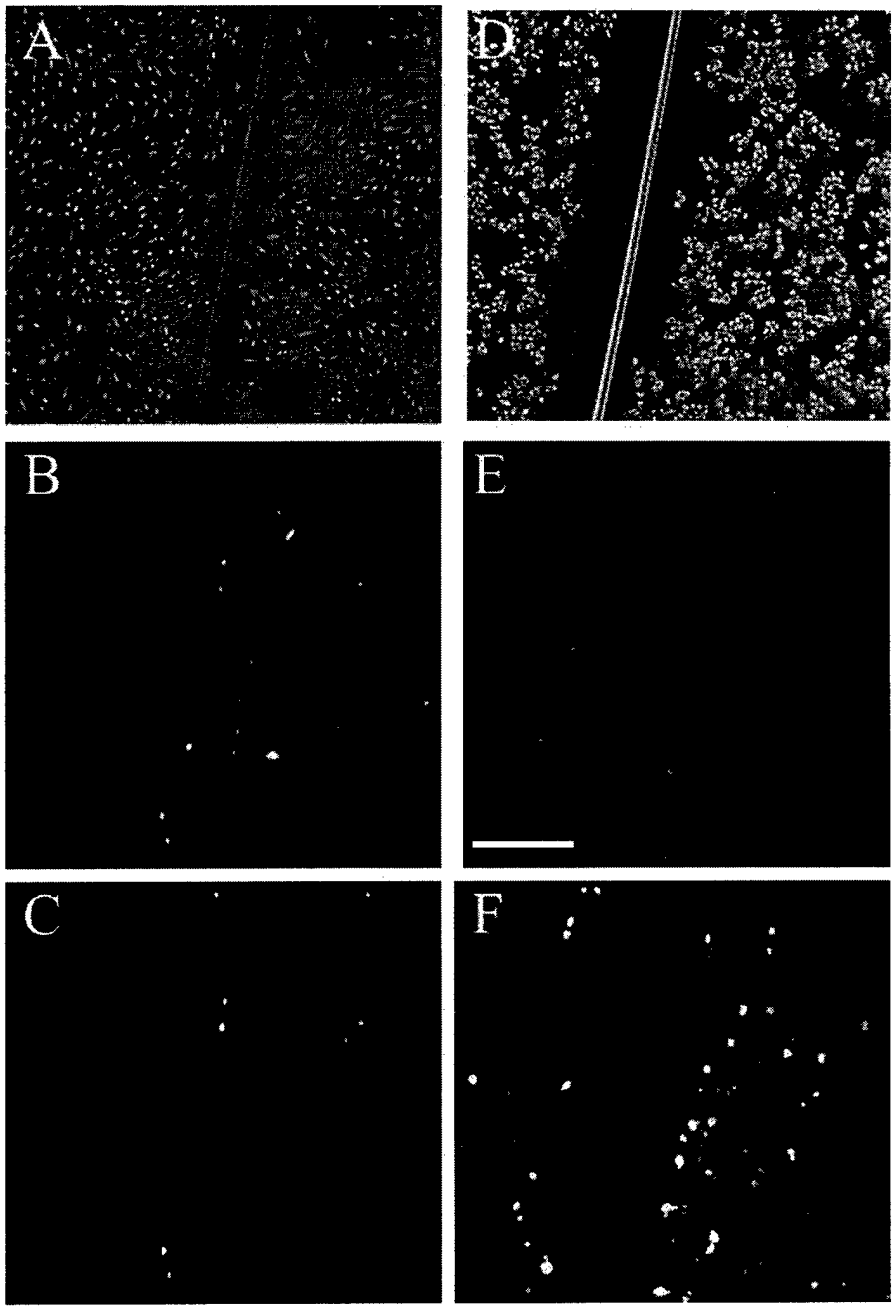

FIG. 6. *BRMS1* transfectants of human melanoma cell lines have restored homotypic gap junctional communication (GJIC). GJIC was evaluated by the scrape loading dye transfer technique. Briefly, cell monolayers were scratched with a 26-gauge needle to load Lucifer yellow dyes. Cells were monitored with a fluorescent microscope (Lucifer yellow, $\lambda_{excitation}$ = 480 ± 20 nm and $\lambda_{emission}$ = 535 ± 25 nm; and rhodamine dextran, $\lambda_{excitation}$ = 535 ± 40 nm and $\lambda_{emission}$ = 610 ± 37.5 nm) and digitally imaged using the Leica DC Viewer, Version 3.2.0.0 (Leica Microsystems Ltd.) (bar, 200 μm). Transfer of Lucifer yellow from loaded cells to adjoining cells indicates functional gap junctions. A representative experiment is shown for MelJuSo vector-only (A–C) and *BRMS1* (D–F) transfectants. A and D, bright field phase illumination; B and E, uptake of rhodamine dextran; C and F, Lucifer yellow. Note: For vector-only transfectants (and parental cells, data not shown), Lucifer yellow did not get transferred to cells separated from the wound. Lucifer yellow fluorescence was observed in *BRMS1* transfectants in cells beyond the scrape-loaded melanoma cells. Similar results were observed for C8161.9 (data not shown).

principle underlying the technique is that a small dye, Lucifer yellow (M_r 457 Da) can be transferred to adjacent cells through functional gap junction channels, while rhodamine dextran (M_r 10 kDa) will not pass through the channels. Melanoma cells along the wound created by scraping with a needle incorporate LY and RD. Examination of the monolayers several minutes later reveals that LY was not transferred in parental, metastatic, vector transfectants (Fig. 6C), but was transferred to adjacent cells in *BRMS1* transfectants of

both MelJuSo (Fig. 6F) and C8161.9 (data not shown). These results confirm and extend to another tumor type the observation that *BRMS1* restores homotypic GJIC concomitant with diminishment of metastatic potential. It is not yet known whether restoration of GJIC is responsible for metastasis suppressor or whether the phenotypes are coincident. Studies are under way to evaluate these alternatives.

In summary, previous studies had mapped melanoma progression-associated genes to the long arm of human chromosome 11. In this series of experiments, we tested whether *BRMS1,* a metastasis suppressor gene originally cloned from breast carcinoma, functioned similarly in malignant melanoma. *BRMS1* does not appear to be the tumor suppressor mapped to chromosome 11q23 previously by Robertson *et al.* [27]; however, it does appear to be a *bona fide* metastasis suppressor in a completely distinct tumor type. The data obtained in these studies do not explain why *BRMS1* suppressed metastasis in C8161 whereas introduction of chromosome 11 did not [11]. Perhaps the level of expression or absence/presence of cofactors in the C8161.9 subclone may be involved.

This findings reported here support the hypothesis that there are shared biochemical and molecular foundations of metastatic potential in distinct tumor histologic types. *BRMS1* is one of a growing number of metastasis regulatory genes. Despite the correlations observed here and elsewhere related to suppression of metastasis, the biochemical mechanisms by which most function remain enigmatic. However, determining how they work offers potential for clinical exploitation.

This research was supported by grants from the U.S. Public Health Service CA 87728 (D.R.W.), CA62168 (D.R.W.), CA90991 (H.J.D./D.R.W.), the U.S. Army Medical Research and Materiel Command DAMD17-00-1-0646 (H.J.D.), the National Foundation for Cancer Research (D.R.W.), and the Jake Gittlen Memorial Golf Tournament (D.R.W.). L.A.S. is supported by a postdoctoral fellowship from the Susan G. Komen Breast Cancer Foundation. R.S.S. is supported by a postdoctoral fellowship (DAMD17-01-1-0362) from the U.S. Army Medical Research and Materiel Command.

REFERENCES

1. American Cancer Society (1998). Cancer Statistics 1998. *CA Cancer J. Clin.* **48,** 1–63.
2. Welch, D. R., and Goldberg, S. F. (1997). Molecular mechanisms controlling human melanoma progression and metastasis. *Pathobiology* **65,** 311–330.
3. Welch, D. R., and Rinker-Schaeffer, C. W. (1999). What defines a useful marker of metastasis in human cancer? *J. Natl. Cancer Inst.* **91,** 1351–1353.
4. Yoshida, B. A., Sokoloff, M., Welch, D. R., and Rinker-Schaeffer, C. W. (2000). Metastasis-suppressor genes: A review and perspective on an emerging field. *J. Natl. Cancer Inst.* **92,** 1717–1730.
5. Robertson, G., Coleman, A., and Lugo, T. G. (1996). A malignant melanoma tumor suppressor on human chromosome 11. *Cancer Res.* **56,** 4487–4492.
6. Seraj, M. J., Samant, R. S., Verderame, M. F., and Welch, D. R. (2000). Functional evidence for a novel human breast carcinoma metastasis suppressor, *BRMS1,* encoded at chromosome 11q13. *Cancer Res.* **60,** 2764–2769.
7. Samant, R. S., Debies, M. T., Shevde, L. A., Verderame, M. F., and Welch, D. R. (2002). Identification and characterization of murine ortholog (*Brms1*) of breast cancer metastasis suppressor 1 (*BRMS1*). *Intl. J. Cancer* **97,** 15–20.
8. Miele, M. E., Robertson, G., Lee, J. H., Coleman, A., McGary, C. T., Fisher, P. B., Lugo, T. G., and Welch, D. R. (1996). Metastasis suppressed, but tumorigenicity and local invasiveness unaffected, in the human melanoma cell line MelJuSo after introduction of human chromosomes 1 or 6. *Mol. Carcinog.* **15,** 284–299.
9. Johnson, J. P., Demmer-Dieckmann, M., Meo, T., Hadam, M. R., and Reithmuller, G. (1981). Surface antigens of human melanoma cells defined by monoclonal antibodies. I. Biochemical characterization of two antigens found on cell lines and fresh tumors of diverse tissue origin. *Eur. J. Immunol.* **11,** 825–831.
10. Welch, D. R., Bisi, J. E., Miller, B. E., Conaway, D., Seftor, E. A., Yohem, K. H., Gilmore, L. B., Seftor, R. E. B., Nakajima, M., and Hendrix, M. J. C. (1991). Characterization of a highly invasive and spontaneously metastatic human malignant melanoma cell line. *Intl. J. Cancer* **47,** 227–237.
11. Welch, D. R., Chen, P., Miele, M. E., McGary, C. T., Bower, J. M., Weissman, B. E., and Stanbridge, E. J. (1994). Microcell-mediated transfer of chromosome 6 into metastatic human C8161 melanoma cells suppresses metastasis but does not inhibit tumorigenicity. *Oncogene* **9,** 255–262.
12. Welch, D. R. (1997). Technical considerations for studying cancer metastasis *in vivo. Clin. Exp. Metastasis* **15,** 272–306.
13. Welch, D. R., and Tomasovic, S. P. (1985). Implications of tumor progression on clinical oncology. *Clin. Exp. Metastasis* **3,** 151–188.
14. Fu, T. M., Bonneau, R. H., Epler, M., Tevethia, M. J., Alam, S., Verner, K., and Tevethia, S. S. (1996). Induction and persistence of a cytotoxic T lymphocyte (CTL) response against a herpes simplex virus-specific CTL epitope expressed in a cellular protein. *Virology* **222,** 269–274.
15. Kierstead, T. D., and Tevethia, M. J. (1993). Association of p53 binding and immortalization of primary C57BL/6 mouse embryo fibroblasts by using simian virus 40 T-antigen mutants bearing internal overlapping deletion mutations. *J. Virol.* **67,** 1817–1829.
16. Bradford, M. M. (1976). A rapid and sensitive method for the quantitation of microgram quantities of proetin utilizing the principle of protein–dye binding. *Anal. Biochem.* **72,** 248–254.
17. Cheng, B., Zhao, S., Luo, J., Sprague, E., Bonewald, L. F., and Jiang, J. X. (2001). Expression of functional gap junctions and regulation by fluid flow in osteocyte-like MLO-Y4 cells. *J. Bone Miner. Res* **16,** 249–259.
18. Herbst, R. A., Mommert, S., Casper, U., Podewski, E. K., Kiehl, P., Kapp, A., and Weiss, J. (2000). 11q23 allelic loss is associated with regional lymph node metastasis in melanoma. *Clin. Cancer Res.* **6,** 3222–3227.
19. Kuramochi, M., Fukuhara, H., Nobukuni, T., Kanbe, T., Maruyama, T., Ghosh, H. P., Pletcher, M., Isomura, M., Onizuka, M., Kitamura, T., Sekiya, T., Reeves, R. H., and Murakami, Y. (2001). TSLC1 is a tumor-suppressor gene in human non-small-cell lung cancer. *Nature Genet.* **27,** 427–430.

20. Plantaz, D., Vandesompele, J., Van Roy, N., Lastowska, M., Bown, N., Combaret, V., Favrot, M. C., Delattre, O., Michon, J., Benard, J., Hartmann, O., Nicholson, J. C., Ross, F. M., Brinkschmidt, C., Laureys, G., Caron, H., Matthay, K. K., Feuerstein, B. G., and Speleman, F. (2001). Comparative genomic hybridization (CGH) analysis of stage 4 neuroblastoma reveals high frequency of 11q deletion in tumors lacking MYCN amplification. *Int. J. Cancer* **91,** 680–686.

21. Ibrahim, S., Estey, E. H., Pierce, S., Glassman, A., Keating, M., O'Brien, S., Kantarjian, H. M., and Albitar, M. (2000). 11q23 abnormalities in patients with acute myelogenous leukemia and myelodysplastic syndrome as detected by molecular and cytogenetic analyses. *Am. J. Clin. Pathol.* **114,** 793–797.

22. Herlyn, M., Kath, R., Williams, N., Valyi-Nagy, I., and Rodeck, U. (1990). Growth-regulatory factors for normal, premalignant and malignant human cells *in vitro*. *Adv. Cancer Res.* **54,** 213–234.

23. Jiang, H., Lin, J., Su, Z., Herlyn, M., Kerbel, R. S., Weissman, B. E., Welch, D. R., and Fisher, P. B. (1995). The melanoma differentiation-associated gene *mda*-6, which encodes the cyclin-dependent kinase inhibitor p21, is differentially expressed during growth, differentiation and progression in human melanoma cells. *Oncogene* **10,** 1855–1864.

24. Kramer, R. H., Bensch, K. G., and Wong, J. (1986). Invasion of reconstituted basement membrane matrix by metastatic human tumor cells. *Cancer Res* **46,** 1980–1989.

25. Albini, A., Iwamoto, Y., Kleinman, H. K., Martin, G. R., Aaronson, S. A., Kozlowski, J. M., and McEwan, R. N. (1987). A rapid *in vitro* assay for quantitating the invasive potential of tumor cells. *Cancer Res.* **47,** 3239–3245.

26. Saunders, M. M., Seraj, M. J., Li, Z. Y., Zhou, Z. Y., Winter, C. R., Welch, D. R., and Donahue, H. J. (2001). Breast cancer metastatic potential correlates with a breakdown in homospecific and heterospecific gap junctional intercellular communication. *Cancer Res.* **61,** 1765–1767.

27. Robertson, G. P., Goldberg, E. K., Lugo, T. G., and Fountain, J. W. (1999). Functional localization of a melanoma tumor suppressor gene to a small (less than or equal to2 Mb) region on 11q23. *Oncogene* **18,** 3173–3180.

Received September 24, 2001
Revised version received November 27, 2001

Li, Zhongyong (1)
Department of Orthopeadic, College of Medicine
, The Penn State University
500 University Dr.
Hershey,PA 17033
U.S.A.717-531-5244 / Fax: 717-531-7583 /
zli@mrl.hmc.psu.edu

Additional Info and Keywords

Tumors;gap junction connexin 43;breast cancer and osteoblastic cell;osteopontin mRNA;metastasis

Disclosure

Donahue
Appendix 4

ABSTRACT NO. _____
PAPER NO. _____

RESTORATION OF CONNEXIN 43 ALTERS BREAST CANCER CELL METASTATIC POTENTIAL TO BONE BY DOWN REGULATION OF OSTEOPONTIN AND CONNEXIN 32

+*Li, Z; *Zhou, Z; **Welch, D R; *and Donahue, H J

+*Musculoskeletal Research Laboratory, Department of Orthopaedics and Rehabilitation, College of Medicine, The Penn State University, Hershey, PA 17033. 717-531-5244, Fax: 717-531-7583, zli@mrl.hmc.psu.edu

Introduction Gap junctions are membrane spanning channels that facilitate intercellular communication by allowing small signaling molecules to pass from cell to cell. Our studies and others suggest that expression of connexin Cx43, a specific gap junction protein, suppresses the cancer phenotype of human mammary carcinoma cells and is correlated with breast cancer cell metastatic potential. Our previous studies also suggested that a breakdown in homospecific (same cell type) and heterospecific (different cell type) gap junctional intercellular communication (GJIC) between breast cancer and osteoblastic cells contributed to breast cancer metastastic potential (1, 2). Osteopontin (OPN) is synthesized and secreted into the extracellular matrix by osteoblasts and has been implicated in cancer migration possibly by serving as a cancer cell chemoattractant. (3) Our previous data suggested an inverse relationship between Cx43 and OPN expression in rat osteosarcoma (ROS) and human fetal osteoblastic (hFOB) cells (4,5,1). Additionaly, Cx43 expression was undetectable in metastatic MDA-MB-435 breast cancer cells (435) whereas OPN and Cx32 expression were upregulated in 435 cells, relative to 435 cells expresing the metastasis expressing gene BRMS-1 or non-metastastic breast epitheliall cells Hs578Brt (Hs578). In this study we examined the hypothesis that restoring Cx43 expression in 435 cells would alter GJIC as well as Cx32 and OPN expression.

Methods 1. **Cx43 plasmid construction and transfection** A 1,710 pb fragment of human Cx43 cDNA was ligated into the Kpn1 and Xba1 sites of pcDNA3.1/hygromycin B(-) (pvcHY). The constructed human Cx43 plasmid ($Cx43^+$) was analyzed using ABI model 377 sequencer. 435 cells were cultured in DMEM-F12 with 5% FBS until 70% confluent. Either 2 μg of $Cx43^+$ or 2 μg pvcHY was transfected into 435 cells using Lipofectamine plus reagent and selected with 350 μg /ml hygromycin B for 10 days to 2 weeks until the resistant colonies [435 transfected with $Cx43^+$ (435/$Cx43^+$) or 435 transfected with pvcHY (plasmid vector control)(435/pvcHY)] were clearly visible. Colonies were trypsinized, passed and maintained with 200 μg /ml hygromycin B. **2. Colony screening** Colonies were screened by northern blot with a human Cx43 cDNA probe and high Cx43 mRNA profile clones were selected as the candidates. **3. Cell to cell communication assay** 435, 435/$Cx43^+$, 435/pvcHY and hFOB were examined for homospecific and heterospecific GJIC using double labeling dye transfer technique. Briefly, donor cells were loaded with two fluorescent dyes, one of which was gap junction permeable and one of which was membrane bound. Communication between cells was determined by dropping donor cells on plates of acceptor cells and counting the number of cells that received the gap junction permeable dye utilyzing fluorescent microscopy. **4. Real time RT PCR** Steady state levels of mRNAs for Cx43, OPN and Cx32 were quantified by real time RT PCR.

Results Sequence analysis indicated that a 1,710 pb fragment of Cx43 DNA was ligated into pcDNA3.1/hygromycin (-). 15 clones of $Cx43^+$ transfetants (435/$Cx43^+$) and 12 clones of plasmid vector control (435/pvcHY) were produced. Real time RT-PCR revealed that Cx43 was detected in all 15 clones of 435/$Cx43^+$ (three of which are shown in figure 1) while Cx43 was undetectable in all 12 clones of 435/pvcHY(one of which is shown in figure 1). Cx43 mRNA levels similar to 435/$Cx43^+$ were detected in hFOB cells and non-metastatic breaet epithelial cells (Hs578). Liver tissue was used as positive control for Cx32 and negative control for OPN. OPN and Cx32 mRNA levels were decreased in 435/$Cx43^+$ cells relative to 435 or pvcHY, but were still greater than in hFOB cells and Hs578. Homotypic GJIC between 435/$Cx43^+$ cells was increased 5 to 8.5 fold relative to GJIC between 435/pcvHY cells. Heterotypic coupling between 435/$Cx43^+$ and hFOB cells increased 1.5 to 3 fold relative to that between 435/pvcHY and hFOB cells (table 1).

Discussion In this study we constructed a human Cx43 expression plasmid and successfully transfected it into 435 cells resulting in 15 435/$Cx43^+$ clones and 12 435/pvcHY (plasmid vector control) clones. We found that restoring Cx43 expression in 435 cells decreased OPN expression, a marker of highly invasive cancer cells, and Cx32 expression, which while expressed in metastatic 435 cells, we had previously shown is undetectable in metastatis suppresed 435/BRMS-1 cells and normal breast epithelial cells (1). Finally, Cx43 expression restored homotypic GJIC between 435 cells, a lack of which is associated with tumorgenic and metastatic potential, and increased heterotypic communication between breast cancer cells and osteoblastic cells. Taken together these results suggest an inverse relationship between Cx43 expression and metastatic potential of breast cancer cells. Furthermore, since breast cancer cells which do and do not express Cx43 appear to express different metastatic potentials and since heterotypic GJIC between these cells and osteoblastic cells differ, we suggest that alteration in GJIC may be related to breast cancer cell metastasis to bone.

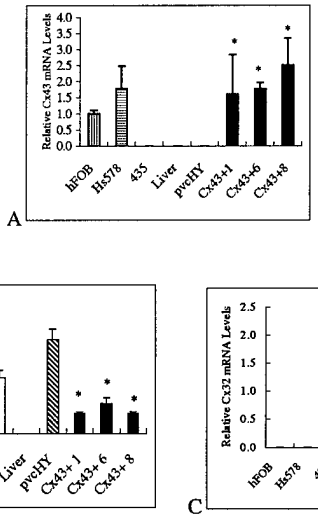

*Figure 1 (A,B,C). Real time RT PCR quantification of steady state mRNA levels of Cx43 (A), OPN (B) and Cx32 (C). RNA was extracted from three 435/$Cx43^+$ clones ($Cx43^+$1, 6 and 8), vector controls (pvcHY), 435 cells, liver tissue (Liver), non-metastatic epithelial cells (Hs578) and hFOB cells. Values are means ±SD. * Sig. Diff. from pvcHY, $p<0.05$, n=3.*

	HOMOTYPIC COUPLING				HETEROTYPIC COUPLING			
Donor	435	pvcHY	Cx43+6	Cx43+8	435	pvcHY	Cx43+6	Cx43+8
Acceptor	435	pvcHY	Cx43+6	Cx43+8	hFOB	hFOB	hFOB	hFOB
Coupling	0.13	0.6	3	5	0.93	9.57	31.57	18.71

Table 1. Homotypic and heterotypic GJIC in breast cancer cells and hFOB cells. Coupling data represent the average numbers of acceptor cells coupled to a single dye loaded donor cell. Data are from at least 110 donor cells for each group.

References

1 Saunders et al *Cancer Research* 61:1765-1767, 2001
2 Hirschi et al *Cell Growth and Differentiation* 7:861-870, 1996
3 Yoneda et al *Eru. J. Cancer* [A]. 34:240-245, 1998
4. Li et al *Bone* 25: 661, 661-666, 1999
5. Li et al *ORS* 2001

* * Jake Gittlen Cancer Insititute

This work is supported by grants from NIH AG 13087, CA90991 and US Army Concept Award

Abstract Status

We have successfully received your abstract, which is displayed below. You will receive a proof of your abstract in late November; please note that you must return your proof with any necessary minor changes by December 10, 2001. Notifications of abstract status will be sent in mid-January 2002.

CONNEXIN 43 TRANSFECTION DECREASES OSTEOPONTIN EXPRESSION IN BREAST CANCER CELLS AND INCREASES THEIR GAP JUNCTIONAL COMMUNICATION WITH BONE CELLS

Zhongyong Li, Zhiyi Zhou, Danny R Welch, Henry J Donahue
Department of Orthopaedics and Rehabilitation and Jake Gittlen Cancer Institute The Penn State University College of Medicine, Hershey PA

Our previous studies suggest that breast cancer cell metastatic potential is correlated with a breakdown in homotypic (same cell type) gap junctional intercellular communication (GJIC). Furthermore, we demonstrated that highly metastatic MDA-MB-435 breast cancer cells (435) express the gap junction protein connexin (Cx) 32 while Cx43 is undetectable. On the other hand, 435 cells expressing the metastasis suppressing gene BRMS1 (435-BRMS-1) express Cx43 but Cx32 is undetectable, a Cx expression profile similar to normal breast epithelial tissue. 435 cells also express abundant osteopontin (OPN), an extracellular matrix protein that promotes breast cancer metastasis to bone, whereas OPN is undetectable in 435-BRMS-1 cells. These data suggest an inverse relationship between Cx43 and OPN expression in breast cancer cell lines, a phenomenon we and others have demonstrated in bone cells. In this study we expressed Cx43 in 435 cells in hope of down-regulating OPN expression and thereby decreasing metastatic potential. We constructed a human Cx43 DNA expression plasmid and stably transfected it into 435 cells resulting in 15 Cx43 transfectant (435/Cx43+) clones and 12 control (435/pvcHY) clones. Northern blot and real time RT-PCR revealed that all 435/Cx43+ expressed Cx43 while no Cx43 was detected in 435/pvcHY. Cx43 mRNA levels similar to 435/Cx43+ were detected in human fetal osteoblastic cells and normal breast epithelial cells. Steady state levels of OPN mRNA were significantly decreased 3-5 fold in 435/Cx43+ cells and Cx32 mRNA levels were decreased 2-3 fold. Finally, Cx43 expression restored homotypic GJIC between 435 cells, a lack of which is associated with tumorigenic and metastatic potential, and increased heterotypic GJIC between breast cancer cells and osteoblastic cells. Taken together, these results suggest a relationship between Cx43 and OPN expression and metastatic potential. Additionly, since highly metastatic cells express greater GJIC with bone cells than do metastasis suppressed clones, we suggest an alteration in GJIC my be related to breast cancer metastasis to bone.